02
2020

BILINGUAL PUBLISHING CO.
Pioneer of Global Academics Since 1984

Volume 3 | Issue 2 | April 2020 | ISSN 2630-5119 (Online)

Journal of Atmospheric Science Research

ISSN 2630-5119
02
9 772630 511201

APSCI
creative commons
CNKI 中国知网 www.cnki.net 中国知识基础设施工程
Google scholar
Crossref
MyScienceWork

Volume 3 Issue 2 • April 2020 • ISSN 2630-5119 (Online)

Journal of Atmospheric Science Research

BILINGUAL PUBLISHING CO.

Pioneer of Global Academics Since 1984

BILINGUAL PUBLISHING CO.
Pioneer of Global Academics Since 1984

Volume 3 | Issue 2 | April 2020 | Page 1-38
Journal of Atmospheric Science Research

Contents

Article

1 **Features of the Three Dimensional Structures in the Pacific Sub-sur-face Layer in Summer**
Luyuan Chen Rong Cheng Feimin Zhang Kai Yang Chenghai Wang

11 **Planetary Layer Lapse Rate Comparison of Tropical, Montane and Hot Semi-Arid Climates of Nigeria**
David O. Edokpa Precious N. Ede

19 **Understanding the Nexus between Climate Change, the Shift in Land Use toward Cashew Production and Rural Food Security in Ghana; the Experiences of Farmers in the Transition Zone of Ghana**
Victor Adjei Moses Ackah Anlimachie Eunice Elorm Ativi

28 **Global Warming and Its Multiple Causes**
Romdhane Ben Slama

32 **Characterization of PM 2.5 Mass Concentration in the Onshore of Sanya, China**
Ping Wang Chao Han Youzhi Zhao Wenci Ding Zengzeng Li

BILINGUAL PUBLISHING CO.
Pioneer of Global Academics Since 1984

Journal of Atmospheric Science Research
https://ojs.bilpublishing.com/index.php/jasr

ARTICLE

Features of the Three Dimensional Structures in the Pacific Sub-surface Layer in Summer

Luyuan Chen Rong Cheng Feimin Zhang Kai Yang Chenghai Wang*

Research and Development Center of Earth System Model (RDCM), Lanzhou University, Key Laboratory of Arid Climate Change and Disaster Reduction of Gansu Province, College of Atmospheric Sciences, Lanzhou University, Lanzhou, Gansu, 730000, China

ARTICLE INFO

Article history
Received: 15 June 2020
Accepted: 27 June 2020
Published Online: 30 June 2020

Keywords:
Pacific sea temperature
Spatial structure
Temporal evolution

ABSTRACT

The anomaly of the summer sea temperature is analyzed by a spatial-temporal synthetically rotated Empirical Orthogonal Function (REOF) at three different depths (0 m, 40 m, and 120 m) over the area 110°E~100°W and 30°S~60°N. The spatial-temporal distribution shows that the "signal" of annual anomaly is stronger in the sub-surface layer than the surface layer, and it is stronger in the eastern equatorial Pacific than in the western area. The spatial structure of the sea temperature anomaly at different layers is related to both the ocean current and the interaction of ocean and atmosphere. The temporal changing trend of the sub-surface sea temperature in different areas shows that the annual mean sea temperature increases and the annual variability evidently increases since the 1980s, and these keep the same trend with the increasing El Nino phenomenon very well.

1. Introduction

Since the El Nino phenomenon has brought to the public's attention, the ocean has attracted more and more meteorologists to pay attention to it. There are many important research results about the ocean and the interaction between ocean and atmosphere. However, most of the research is based on the observed sea surface temperature (SST) or the analysis of the single layer ocean. On the whole, there is not only the horizontal, but also the vertical exchange in the ocean. It is indicated that the annual vertical temperature gradient is much larger than that in the horizontal direction. Therefore, vertical structure of ocean should be paid more attention when analyzing the distribution of ocean temperature [1]. The mechanism for the various warm-pool anomalies in the western Pacific has indicated that the warm-pool sub-surface sea temperature anomaly in the western Pacific which plays important role in the El Nino event, since it connects closely with the western passing of the northern equatorial current temperature's abnormal signal. It has been proven that the warm-pool abnormal warm water in the western Pacific mainly comes from northern equatorial current, which is aroused by the subduct of surface warm water in the Middle East Pacific along with the thermocline, which can reach up to 120 m in the area of warm pool in the western Pacific. During the period between the end of the El Nino event and the onset of the La Nina event, the sub-surface abnormal warm water in the northern equatorial current area (in the vicinity of 10°N) spreads from

**Corresponding Author:*
Chenghai Wang,
Research and Development Center of Earth System Model (RDCM), Lanzhou University, Key Laboratory of Arid Climate Change and Disaster Reduction of Gansu Province, College of Atmospheric Sciences, Lanzhou University, Lanzhou, Gansu, 730000, China;
Email: wch@lzu.edu.cn

 DOI: https://doi.org/10.30564/jasr.v3i2.1999

the Middle East Pacific to the western Pacific warm pool subduct along with the thermocline, and the abnormal warm water signal increases and extends, and finally the warm water controls the whole western Pacific, and provides the essential conditions for the onset of an El Nino event [2]. Results of Chao et al (2002) showed that the initial ocean temperature departure of El Nino or La Nino aroused by the observation mainly appeared in the thermocline at about 150 m in a warm pool; when its intensity reached up to a specific threshold, it would spread to the tropic western Pacific along with climatic thermocline and move up to the sea surface. In the western boundary of the Pacific, the anomalies forced by the atmosphere can arouse sub-surface temperature anomaly, which spreads to the ocean east, mainly with an east-spread Kelvin wave, and arouses the anomaly in the whole ocean [3]. The sea temperature in the upper layer tropical Pacific Ocean has shown that there is a relationship between the various features of ocean surface in the area of the western Pacific warm pool (0-16°N, 125-145°E) and the sub-surface ocean temperature in the western direction. It is discovered that there is a remarkable annual anomaly of vertical temperature in the western Pacific warm pool, with the most evident area appears in the sub-surface (120-200 m). The sub-surface change signal of temperature in the western Pacific "warm pool" is clearly earlier than the ocean temperature's anomaly in the western Pacific sub-surface. The sub-surface ocean temperature in Pacific "warm pool" area has a pronounced inter-annual anomaly, and there was negative departure during the El Nino period and positive departure during the La Nino period in the warm pool area. The sub-surface sea temperature departure in the warm pool area has a distinct decreasing trend and the descending rate of the temperature is -0.2°C/10a. During the ENSO cycle, the anomaly signal of the sub-surface sea temperature in the equatorial western Pacific appears firstly in the warm pool area, and the abnormal signal becomes much stronger and then spreads to the east and the equator, finally it spreads to the surface (under the force of the atmosphere) from the equatorial western Pacific to Middle East Pacific along with thermocline when the intensity reaches up to a specific threshold. The period of diffusion perhaps needs 18 months, in other words, the sub-surface abnormal signal of the sea temperature in warm pool is an important condition for the anomaly of the ocean temperature field in the western Pacific. Therefore, the anomaly of sub-surface ocean temperature in the warm pool area is essential for the occurrence of an El Nino event or La Nina event[4]. Chao et al assumed that the profound mixing layer (has a large thermal capacity) is connected with the feeble interaction of atmosphere. Some studies also showed that the sub-surface sea temperature in Pacific orderly come through an evident inter-decadal eruption from up to down in around 1980 [4].

Recently, the sea surface is of increasing interest for meteorologists because the annual signal in the deep layer is stronger than the surface layer. Zhang et al. studied the three dimensional structure of sea temperature at the sub-surface and the characters of decadal evolution of changing rate in the northern Pacific, they suggested that anomaly of sub-surface temperature circumgyrated deasil round the subtropical vortex go with average circumfluence. It is evident that this signal is connected with the subduct of temperature anomaly in the "window" area of middle latitude, and this feature especially reflects the action of the Rossby wave. The analyses on isopycnal surfaces reveals two preferential paths of temperature variability which rounding subtropical vortex on the decadal scales, where one is the southwest subduct path derived from the east of northern Pacific center, and another is the subtropical path derived from the east of subtropical to tropical and boundary towards west [5-7].

Above and other researches [8-12] shows that sub-surface sea temperature changes are closely connected with surface temperature change in the Pacific, and the vertical ocean temperature change and distribution are closely connected with El Nino and La Nina [13-17].

The next section provides information on the data and method. Section 3 mainly discusses the three dimensional spatial character of sea temperature in Pacific. The temporal evolution of summer sea temperature in Pacific is analyzed in Sections 4. Conclusion and discussion are given in the final section.

2. Data and Method

2.1 Data

The monthly mean sea temperature comes from the ocean laboratory of environmental data analysis center (JEDAC) of American Scripps [18-19], with the period of January 1995 to December 1998, and the area of 60°S-60°N, 0°-360°. The spatial resolution of the sea temperature is5°×2°, and the vertical layers are 0 m, 20 m, 40 m, 60 m, 80 m, 120 m, 160 m, 200 m, 240 m, 300 m, 400 m, respectively. The layer used in this study is 0, 40 and 120 m, respectively, and the area is from 110°E to100°W, and from 30°S to 60°N.

2.2 Method

In order to analyze the three dimensional structure of multi-layer sea temperature, the spatial-temporal integrated REOF is used in this study. Supposing the data matrix

DOI: https://doi.org/10.30564/jasr.v3i2.1999

of the average sea temperature departure field at L layer is $F^{L}_{N\times M}$, N is the number of temporal sample and M is the number of spatial grid. We turn every layer data into a new matrix:

$$F^{L}_{N\times M} = \{F^{1}_{N\times M} F^{2}_{N\times M} \cdots F^{L}_{N\times M}\} \quad (1)$$

Count its real symmetry matrix:

$$S^{L}_{M\times N} = F^{L}_{M\times N} \cdot F^{L}_{N\times M} \quad (2)$$

The sub-matrix $S_{ij} = F^{i}_{M\times N} \cdot F^{j}_{N\times M}$ is the covariance of i layer and j layer in isobaric surface of monthly mean sea temperature departure field, when i=j, S_{ij} becomes surface of monthly mean temperature departure field, when i=j, S_{ij} becomes the self covariance matrix of monthly mean sea temperature departure field in i layer, so the real symmetry matrix, not only contents the self distributing information of each layer's temperature anomaly, but also the information of interconnection of each layer's temperature departure. Because of the rationale of EOF, the eigenvector of real symmetry matrix $F_{N0\times M}$composes the basic field of matrix$F_{N\times M}$, and also includes the inter-actional information of each layer's temperature departure.

The original material matrix is analyzed by using the mathematical method:

$$F^{L}_{N\times M} = \sum_{K_0} T_{N\times K_0} \cdot V^{L}_{K_0\times M} \quad (3)$$

K_0 is the truncated wave number. If we have the eigenvector of former i, the precision of variance fitting using EOF is:

$$Q_{(K_0)} = \sum_{k=1}^{K_0} \lambda_k \Big/ \sum_{k=1}^{M} \lambda_k \quad (4)$$

(λ_k is the corresponding eigenvalue of the k_{th} eigenvector)

In Eq. (3), $T_{N\times K0}$ is the temporal coefficient matrix of EOF, which includes the character of temporal evolvement of each layer's whole structure anomaly field, where $V_{K0\times M}$ is the eigenvector matrix of EOF, and it can be taken apart in several sub-blocks:

$$V^{L}_{K_0\times M} = \{V^{1}_{K_0\times M} V^{2}_{K_0\times M} \cdots V^{L}_{K_0\times M}\} \quad (5)$$

Every sub-block represents the distributing structure of spatial function of some eigenvector in L layer. In this work, N=45, L=3, LM=3118.

In order to highlight the regional feature of sea temperature anomaly, rotating orthogonal analyzing method (REOF) is used to EOF [20], rotating each two spatial vectors in order in the time of rotating, the factors that are rotated are made certain according to astringency (using the former tenth weight in here), the rotating can be repeated, finally making every rotating total variance to get to the maximum. In the actual calculation, we can study the critical value as the end of adjusting spatial function; we rotate the former tenth vector in our work.

The advantage of this method is that orthogonal function outspread can turn the spatial dot from high dimension down to low dimension, and compress and centralize the spatial-temporal information. Meanwhile, through transforming different elements' field matrix, the matrix includes the information of different elements' field in the temporal and spatial. The eigenvector field obtained using Experience Orthogonal Function (EOF) transformed matrix not only includes the spatial-temporal feature of some elements, but also includes the interaction of the different elements' field. Because the rotating calculation is made on the basis of vector space obtained by the EOF, the RLV of REOF can better reflect the regional features [21].

3. The Three Dimensional Spatial Character of Sea Temperature in the Pacific

Table.1 shows that the astringency of summer sea temperature in the Pacific is slow, it carries the complexity of sea temperature annual change in three-dimensional spatial. The eigenvector obtained by REOF mainly centralizes on the first 4 weights, thus only the spatial structures of the first 4 eigenvectors' are analyzed in this study.

Because of the area which absolute value is larger and has more contribution to the variance, the spatial function of each eigenvector only works when analyzing and discussing an area with a large value. In the following sections, our discussion will focus on analyzing the character of spatial distribution and annual change in an area with a large value (which is called the sensitive area, the absolute value $\geq \alpha_{0.01} \approx 0.37$ in this paper).

Table 1. fitting variances of the first 9 eigenvectors of the departure fields

Order number	1	2	3	4	5	6	7	8	9	∑
RLV	15.0	9.9	7.0	4.4	4.0	3.3	3.0	2.9	2.9	52.4

The sea surface over the middle to east equatorial Pacific is the area where the RLV1 is positive and large. The large value area has more attribution and is the most sensitive area of the annual abnormal change. The positive largest value is at 170°W-140°W, 0-10°N. The RLV1 occupies more than 80% of the annual change variance of the sea temperature in this area, which is the most sensitive area of surface sea temperature annual change

 DOI: https://doi.org/10.30564/jasr.v3i2.1999

in Pacific, and this area is relatively the same as the area where El Nino occurs (Figure 1.a). There are two extreme negative centers; one is centered at the middle to east Pacific (30°N, 170°W-150°W) and another is centered at the zonal area from Indonesia to the northern Australian sea area. The annual change in the area of the east equatorial Pacific changes oppositely with the sea temperature in the area of the western ocean, which is centered at the warm pool and the middle to northern Pacific.

The sea temperature distribution at the depth of 40 m basically has the same characteristic as the sea temperature's annual change (Figure 1.b). The area that has the largest annual change is basically the same as the surface in the spatial distribution, which shows that the deep sea temperature's change is mainly influenced by the surface.

With the increasing of depth, the influence of ocean surface decrease at the depth of 120 m, and the distribution of sea temperature inter-annual variations is obviously different compared to that at 0-40 m. Firstly, the positive value area of middle to west Pacific in 0 m turns to the southeast, the center is on the sea area of the equatorial south. Secondly, the intersecting area between west wind drift and the ocean current of California is the area which has larger annual various, and so we should pay more attention to the warm pool area of the eastern ocean surface in Philippines which is the sensitive area of opposite interannual change, i.e., there is a negative center in the area 10°N, 140°E-150°E, and which is connected with eastern positive changing area that forms the 'Seesaw' which forms along in a quasi-east-west direction.

By analyzing the three layers' sea temperature change, we discover that each horizontal layer's sea temperature change presents the most sensitive area of interannual anomaly of sea temperature in the area of southeast Pacific and north Pacific, which is similar to the SST distribution of El Nino. At the deeper layer of 120m, the interannual anomaly feature has the opposite phase change of northwest-southeast in the equatorial south and north. The annual anomaly of northern west wind drifts and the Californian warm current is another sensitive area that should be paid more attention to. The "signal" of the annual anomaly of Sub-surface sea temperature which a reverse phase change in east - west direction at 120m can transfer upwards under some conditions, but it is not obvious at an under sea level of 120m; that is to say, the "signal" of annual anomaly in eastern Pacific appears earlier in sub-surface than in surface, and the annual anomaly signal of El Nino happens earlier in sub-surface. Hence, in other words, although the area of warm pool has a higher average of sea temperature than any other ocean area in surface, because it is adjusted by factors, such as wind, and exchanges the energy between ocean and atmosphere, it is relatively stable. The annual anomaly in the eastern Pacific is larger. The annual anomaly of surface temperature in eastern area of Pacific is larger at the depth of 120m.

The first eigenvector of REOF frankly reflects the inward relationship of the sea temperature departure field in different layers (Figure 1). We can restrainedly infer the ocean temperature vertical variations by the spatial distribution of three layers' sea temperature, the physical character of seawater in surface is relatively uniform, and the annual anomaly's spatial difference of sea temperature is also relatively homogeneous. The sea temperature has the character of nearly barotropity in the vertical, while the depth is more than 120 m and the character is a similar baroclinity. The sensitive area of sea temperature's annual anomaly indicates the southern excursion commencing from up to down, the homodisperse decrease, and the change is of an opposite phase change in an east-west direction which reflects the circumfluence of sea water exchange existing in deeper sea temperature.

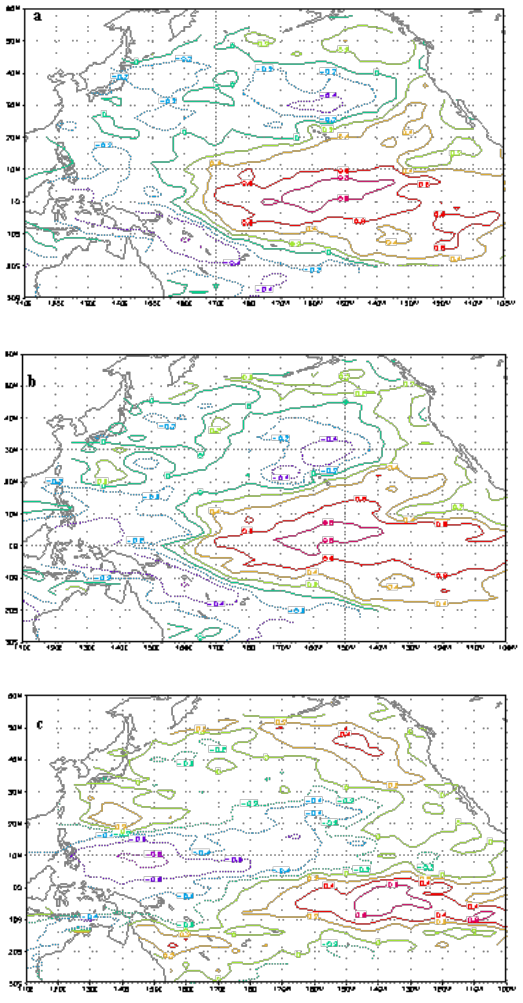

Figure 1. The first eigenvector's distribution (RLV) in (a) 10 m, (b) 40m, and (c) 120 m

DOI: https://doi.org/10.30564/jasr.v3i2.1999

Figure 2 shows the spatial structure of every layer's sea temperature corresponding to the second eigenvector. Figure 2.a shows the sensitive area of annual anomaly on surface which has two main waves, the oscillation between the Kuroshio and the west wind drift shows opposite annual phase change in the two areas; another wave transforming along the direction of east-west shows an annual oscillation in the southeastern Pacific and in large areas of middle to east Pacific, the latter is stronger than the former. The transforming direction of wave at 40m is basically the same as that over the surface fig.2b, and the all sensitive area of annual anomaly sea temperature has the same position and distribution as Figure 2.a. It hardly superposes with Figure 2a in the sea area of the equatorial south; the annual anomaly in the area of west wind drift is relatively weaker, its position is further south, and its area relatively decreases, which reflects the shallow feature and the vertical baroclinity of west wind drift. That is, the vertical amplitude of wave in the direction of east west is large and relatively stable. The feature of middle-west Pacific in southern equatorial at 120m is that sensitive area of annual anomaly retreat to the east equatorial Pacific, the area becomes smaller (set the 0.4 as boundary), and the annual anomaly in the region of eastern Pacific and Kuroshio has already become weaker compared with the surface and sub-surface.

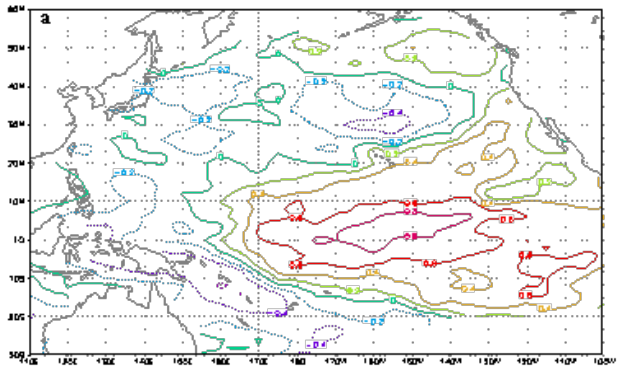

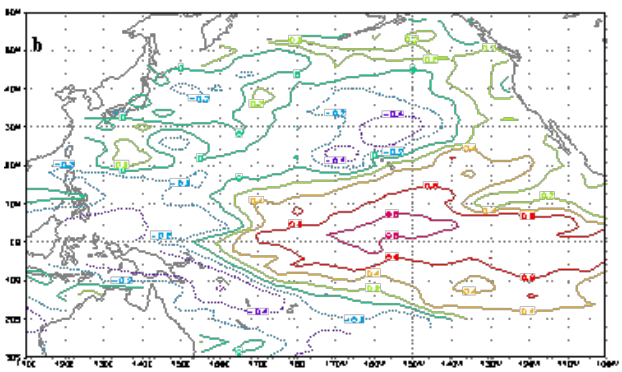

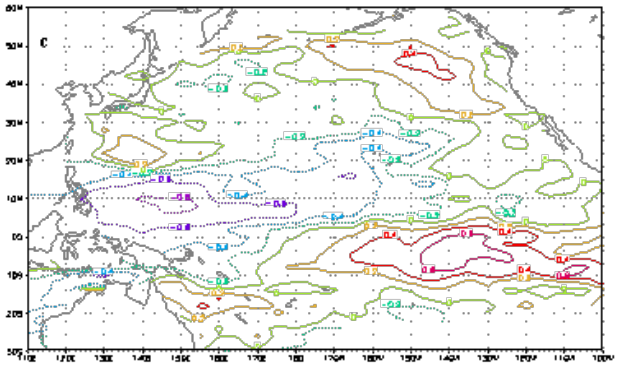

Figure 2. Similar to Figure 1, but for the second eigenvector

It is still nootable that there is an interannual anomaly sensitive area of symmetry distributing in a horizontal direction of sub-surface in this set of charts. Especially the sea temperature change has an opposite phase between the east equatorial Pacific and west Pacific, connected with Walker circulation, warming water area located near Indonesia and the west Pacific equatorial, and the sea temperature is lower in east equatorial Pacific. We can find a similar result with the first eigenvector in the vertical structure, and there is barotropic character in sub-surface.

Figure 3 is the third eigenvector of sea temperature's spatial structure. The feature is that there is a wave transforming in the direction of south-north and the main changing area is north of the Pacific. The main sensitive area of the sea surface is centralized in the northern equatorial area (Figure 3), and the sensitive area of temperature's inter-annual anomaly appears + -- - -- + symmetry distributed along from the north to south. The distribution of sea temperature at the 40m layer (Figure 3.b) has a similar situation with above the sea surface. We can also find the symmetric distribution of the sensitivity area; however, the annual anomaly of west wind drift becomes a little stronger. At the 120m layer (Figure 3.c), there is still a wave transforming in the direction of north to south, but the spatial scale is relatively small and the sensitive area of temperature's interannual anomaly is quite random, every large value's area of sea temperature's interannual anomaly clearly reduces compared with the former two layers, but we can also find the same distributing pattern of sensitive area with the first two layers in the ocean surface of the Northern Hemisphere. Simultaneously, the spatial area of wave transforming expands to the south, that is to say the scale of wave transformation becomes small, but the transforming range becomes large at 120m.

 DOI: https://doi.org/10.30564/jasr.v3i2.1999

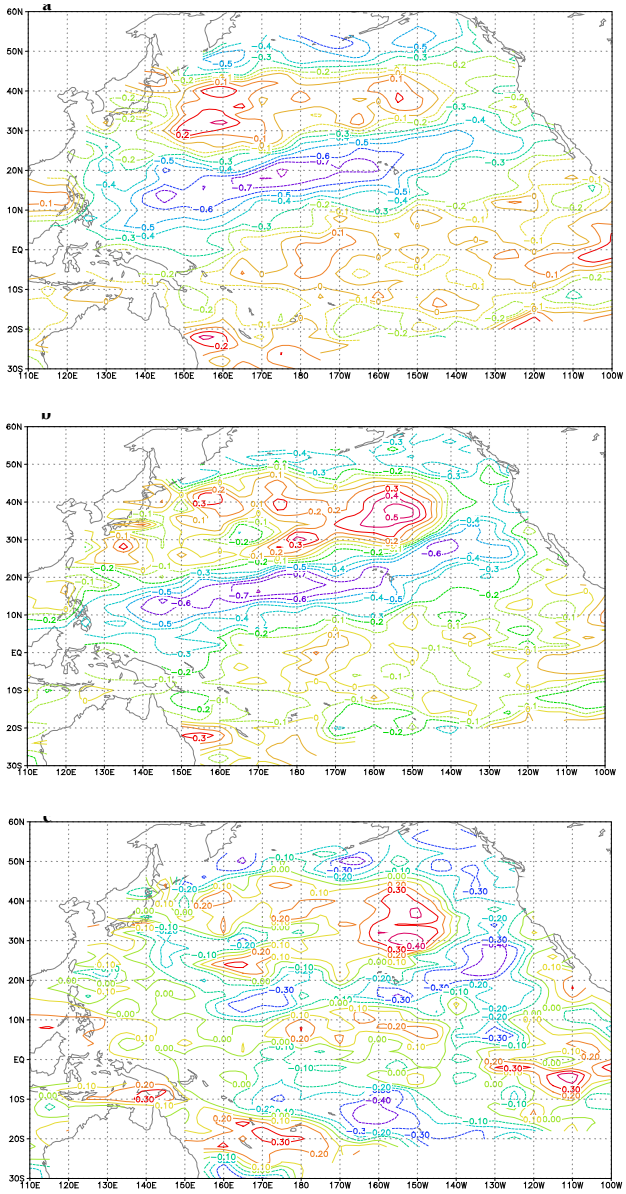

Figure 3. Similar to Figure 1, but for the third eigenvector

Along section of south - north, the sea temperature's change in the area of the tropical and subtropical Pacific has a connection of an opposite phase with a sea temperature change in the area of middle or high latitude of Pacific. This pattern of 'Seesaw' along the section of south to north inosculates with the NPO and also indicates the close relation between sea temperature's field and the field of air pressure.

The sensitive area of the western equatorial Pacific is represented more clearly in the three layers in the fourth eigenvector of the sea temperature's spatial distribution (Figure 4). Because of the influence of the warm equatorial ocean stream, the warm water accumulates in the area of the west equatorial Pacific and forms the ocean area that has the highest average whole Pacific sea temperature, which is called the 'warm pool' area. The sensitive area of sea temperature's interannual anomaly represented by the fourth eigenvector corresponds well to the position of "warm pool". We can discover from Figure 4 that the position of the warm pool in the shallow ocean area and the influenced area does not change too much, while the anomaly area is separated into two parts at the deeper layer of 120m, the southern equatorial part expands to the east and that reflects the existence of different ocean stream exchange; that is to say, the discord caused by the characteristic and property of sub-surface and surface's ocean stream, brings the change of the sea temperature's distribution in up and down.

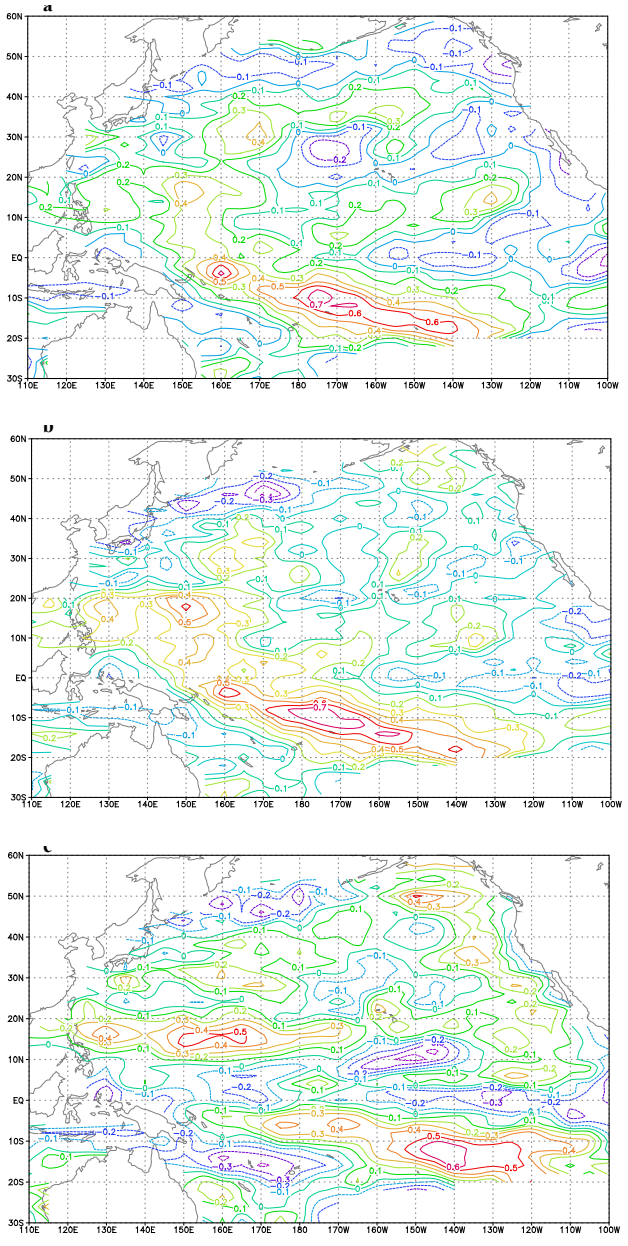

Figure 4. Similar to Figure 1, but for the fourth eigenvector

DOI: https://doi.org/10.30564/jasr.v3i2.1999

Based on the above analysis, the spatial distribution of the sea temperature's structure in Pacific is not only closely related to the action of ocean stream, but also to the atmospheric circulation. The position and distribution of the sensitive area of the sea temperature in surface and sub-surface correspond well with that of ENSO, NPO and Walker circulation, which shows the interaction between the ocean and the atmosphere.

The first four eigenvectors reveal almost the total structure of the barotropy of the subsurface sea temperature field. This barotropy will be replaced by the baroclinity when the depth increases and reached to some level.

4. Temporal Evolution of Summer Sea Temperature in Pacific

Studies have shown that the interannual anomaly of sea temperature has increased evidently since 20th century, especially in middle to east Pacific, and the annual variability is still at the high stage since 1980s from the changing trend [4,22-25]. In order to analyze the temporal evolution of the summer sea temperature, the most sensitive area of the annual sea temperature anomaly in different layers is chosen in this study, the regional average is used to indicate the average sea temperature of this area. Figures 5-7 is the curve of average sea temperature change and the 2 orders fitting in different layer of the sensitive area. Meanwhile for a better compare and analysis, a sensitive area on every layer is made the most same at Ocean region, and represents the east equatorial Pacific, middle Pacific and west Pacific.

From Figures 5-7, it can be seen that the sea temperature in Pacific shows the opposite phase's change in the part of south and north. The SST in east equatorial Pacific shows a decreasing trend from the 1950s to the middle of the 1960s; it turns back in the 1970s and gets to the highest value in the end of the 1980s; there also appears to be a down trend in the1990s. Figure 5.a shows that the surface temperature in western equatorial Pacific has had an increasing trend since the 1980s and annual anomaly bigger significantly. This feature is also appears in another corresponding ocean area, where some research has shown that the frequency of El Nino happens become frequently and its strength stays in the bigger moment from the 1980s to 1990s. [4] So we infer that the change of sea temperature closely connects with the frequency of El Nino; sea temperature change has the opposite trend between middle of northern Pacific and east Pacific equatorial (Figure 5.b), there is a trend of high-low-high. In the area of southwest Pacific, the changing trend of sea temperature presents a persistently increasing trend and the interannual variability is smaller (Figure 5.c).

Comparing Figure 5 with Figure 6, it is found that the changing trend of sea temperature is opposite in the western equatorial and in southeast of the Pacific, being similar with the surface sea temperature, and the amplitude of sea water's temperature of interannual change becomes significantly large since the 1980s, while the changing trend of temperature in west or south of ocean is opposite to that in the area of east Pacific.

Comparing Figure 5 with Figure 6, an opposite trend occurred between the west Pacific's SST and southeast. Similar to SST, Ocean temperature annual anomaly amplitude was larger after 1980. An opposite change trend occurred between the southern area and west Pacific.

The annual sea temperature change in the tropical ocean area (Figure 7a) of the western equatorial Pacific at the depth of 120 m since the 1980s becomes significantly high and its changing trend is similar with that over the surface and at 40m, which reflects the increasing sea temperature's interannual variability in the deeper layer since the 1980s, there is a increasing trend. It is the most sensitive and most remarkable area of Ocean temperature anomaly in the area of northern Pacific. For the middle Pacific (Figure 7.b), the change of sea temperature similar to the sine function form, and the sea temperature is at its peak in the 1960s and the middle of 1990s. In the tropical ocean area of the southeast Pacific (Figure 7c), the changing trend of sea temperature is opposite to that of the surface, furthermore the interannual variability begins to increasing from the 1970s.

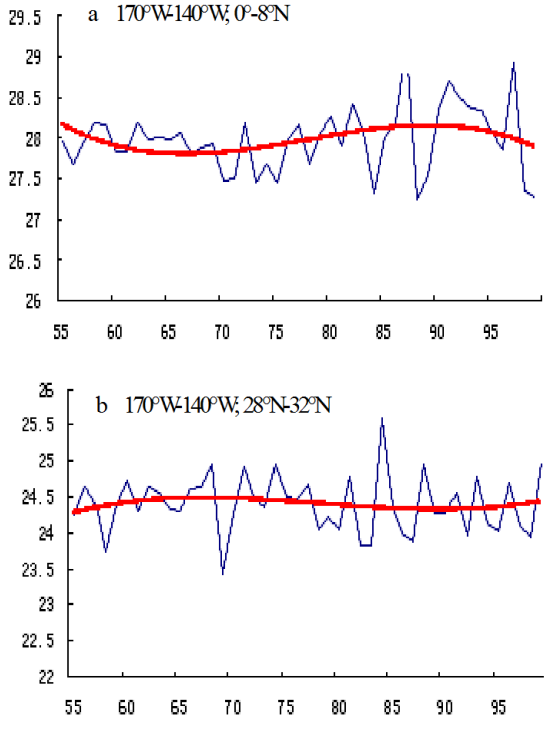

 DOI: https://doi.org/10.30564/jasr.v3i2.1999

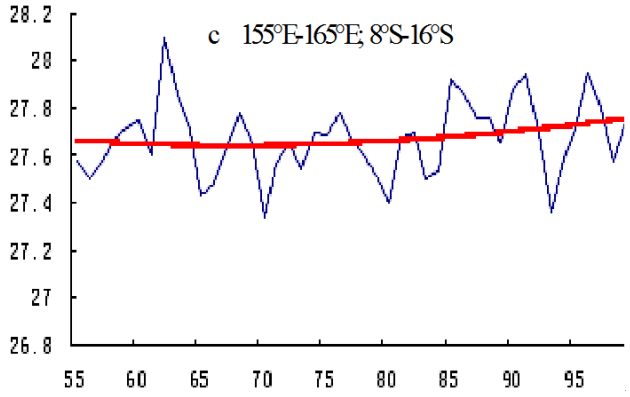

Figure 5. Annual variations of the sea surface temperature in the sensitive area such as (a) 170°W-140°W; 0°N-8°N, (b) 170°W-140°W; 28°N-32°N, and (c) 155°E-165°E; 8°S-16°S

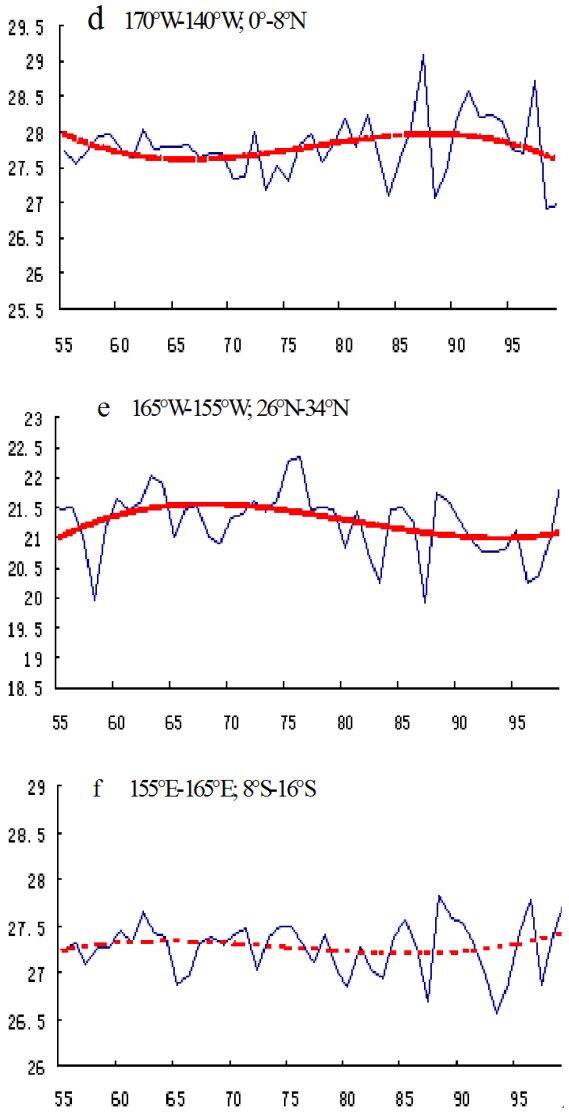

Figure 6. Similar to Figure 5, but for sea temperature at 40 m

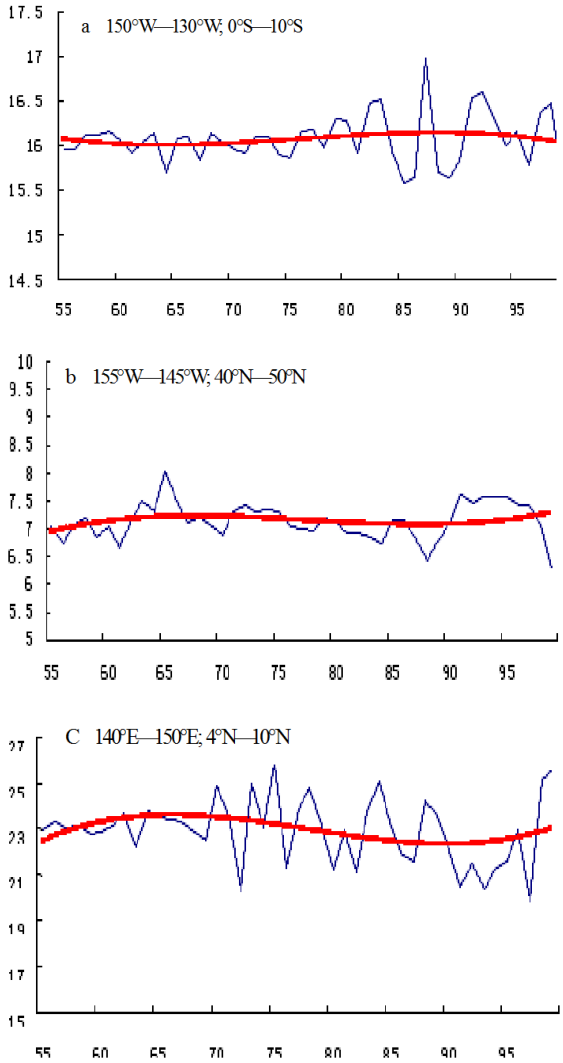

Figure 7. Similar to Figure 5, but for sea temperature at 120 m in the regions of (a) 150°W-130°W; 0°-10°S; (b) 155°W-145°W; 40°N-50°N; (c) 140°E-150°E; 4°N-10°N

5. Conclusion and Discussion

In this study, the anomaly of monthly mean sea temperature over the past 45 years in three layers in the ocean area of northern Pacific is analyzed using the spatial-temple synthesis method. The conclusions are summarized as follows:

(1) The most sensitive area of the annual sea temperature change is in the middle to east equatorial Pacific, where the change can reach down to 120 m below sea level, but the spatial range becomes marginal from sea surdace down to the deeper sea; while the annual mean sea temperature and its range change are relatively weak in west Pacific. The annual mean sea temperature change in sea surface in the west Pacific area (warm pool) clearly becomes larger than that at 120 m and has the opposite

DOI: https://doi.org/10.30564/jasr.v3i2.1898

phase with the east Pacific; the observation shows that the initial departures of the sea temperature producing El Nino or La Nina mainly appear in the thermocline at about 150 m of 'warm pool', when developing to specific threshold, it transforms to the area of east tropical Pacific along with the climatic thermocline and ascends to the surface. The abnormality forced by atmosphere in western boundary of Pacific can cause abnormal temperature in the subsurface and mainly transforms to the east ocean along with the east passing Kelvin wave, finally it leads to the abnormality of the whole Ocean. Therefore, the changing relation of the opposite phase of the abnormally sensitive area of interannual change between west and east equatorial Pacific is the remarkable trait in the northern Pacific.

(2) The sea temperature change in middle to east equatorial Pacific is related to the opposite phase in west equatorial Pacific, which is the basic and main characteristic not only in the sea surface, but also in the whole sub-surface.

(3) The sensitive area of the sea temperature in Pacific changes in different layers can better reflect the general trend of sea temperature in different sea layers. The Sea surface, which is affected by the east and west wind and is adjusted by the change of atmospheric circulations, presents evident uniformly. Meanwhile, the inter-annual abnormal signal of sea temperature in sub-surface can provide better signal to the circulation of ENSO.

(4) The inter-annual change of sea temperature shows an increasing interannual rate from the 1980s to the middle 1990s in the ocean's surface and at 40 m below sea surface level, the increasing trend inosculates with the high frequency of El Nino. Thermocline presents the opposite change with the surface at a depth of 120 m. The break of interannual signal in the Pacific not only exists in the atmosphere and ocean's surface, but also exits in the whole subsurface.

Acknowledgments

This study is supported by the National Science Foundation of China (91837205, 41805032, 41975111).

References

[1] Zhang, C., J. Qi, J. Zuo, F. Zhang. The three dimensional numerical simulation of thermocline in Yellow Sea and Bohai Sea, Acta Oceanologica Sinica, 1997, l9(6): 12-20.

[2] Hui, x., J. Chen, Y. He, L. Xu, G. Song. Sub-surface ocean temperature anomalies in the western Pacific and the anomalous ocean temperature west wars transferring in the north equatorial current, Advance in Waterscience, 2002, 13(2): 133-140.

[3] Chao, J., X. Chen, J.He. The baroclinic response of west tropical Pacific to wind stress, Chinese Journal of Ceophysics, 2002, 45(2):176-187.

[4] Chen, J., Y., He, S., Sun, L., Xu, G., Song, Y., Zhang. The west Pacific warm pool variation and its influence on subsurface ocean temperature field in the West Pacific, Acta Oceanologica Sinica, 2002, 24(3): 35-44.

[5] Zhong, S., J. He, X. Liu. Decadal variability and abrupt change of upper-ocean temperature in the Pacific, Journal of Nanjing Institute of Meteorology, 2002, 25(5): 595-602.

[6] Zhang R. H., S.Levitus. Structure and cycle of decadal variability of upper-ocean temperature in the North Pacific, J. Climate, 1997, 10(4): 7l0-727.

[7] Chen J., G. Song, J. Chu, L. Xu. Oceanic temperature anomalous signal path way in the equatorial Pacific, Advance in Waterscience, 2003, 14(2): 152-157.

[8] Chao J.P., The dynamics of El Nino and southern oscillation, Meteorological press, China, Dec. 1993,167-265

[9] Levitus S., A. H. Orto. Global analysis of oceanographic data, Bull., Am., Meteor., Soc., 1977, 58: 1270-1284.

[10] Bryan K., M.D. Cox, A numerical investigation of the oceanic general circulation. Tellus. 1967, 19: 54-80.

[11] Bryan K.. Pole ward heat transport by the Ocean: observations and models. Annu. Rev., Earth Planet.Sci., 1982, 10: 15-38.

[12] Bryan K.. Climate and the ocean circulation, The ocean model, Mon., Wea, Rev., 1969, 97: 806-827.

[13] Zhao Q., Y. Li, S. Peng. The relationship of between upper sea temperature in Pacific near equator and. The study on observation, simulating and diagnosing of interaction of sea-atmosphere over west tropic Pacific. Beijing, China Meteorological Press, 1996: 35-44.

[14] Chao J., Z., Wang, The simple interaction of Air-sea coupled waves-Rossby waves. Acta Meteorologica Sinica, 1993, 51(4): 385-393.

[15] Gu D.F., S.H. Philander, Inter-decadal climate fluctuations that depend on exchanges between the tropics and extratropics, Science, 1997, 275(5301): 805-807.

[16] Meller G. L., P. A. Durbin, The structure and dynamics of the ocean surface mixture layer, J. Phys. Oceanography, 1975, (5): 718-728.

[17] Lin Chuanlan, Some features of heat content changes of the oceanic upper layer in northwest Pacific during 1964-1982, Tropic Oceanology, 1990, 9(2): 78-85.

[18] White W. B., S.E. Pazan, G. W. Withee, C. Noe, Joint environmental data analysis (Jeda) center for scientific quality control of upper ocean thermal data

 DOI: https://doi.org/10.30564/jasr.v3i2.1999

in support of TOGA and WOCE. EOS Transaction, American Geophysical Union, 1988, 69: 122-123.

[19] Meyers, G., L. Pigot. Analysis of frequently repeated XBT lines in the Indian Ocean. CSIRO Marine Laboratories.Technical Report, 2000, 238: 43.

[20] Horel D.. A Rotated principal Component analysis of the interannual Variability of Northern Hemisphere 500hpa high filed, M. W. R., 1981.

[21] Jin L., B. Zhang, J. Chou. The synthesis analysis on vertical structure of the monthly mean circulation anomalies over the northern hemisphere, Science Atmospheric Sinica, 1993, 17(3): 310-318.

[22] Nitta T, S. Yamada. Recent warming of tropical sea surface temperature and its relationship to the Northern Hemi-sphere circulation. J. Meteor. Soc. Japan, 1989, 67 (3): 375-383.

[23] Levitus S.. Annual cycle of temperature and heat storage in the world ocean. 1984, J., Phys., Oceanogr.

[24] Graham N., E., T. P. Barnet, R. Wilde, et a1, On the roles of tropical and mid-latitude SSTs in forcing interannual to inter-decadal variability in the winter Northern Hemispheric circulation, J. Climate, 1994, 7(8): 1416-1441.

[25] Zhang Y., J.M.Wallace, D.S. Battisti, ENSO-like decadal-to-century scale variability: 1900-l993. J. Climate, 1997, 10(5): 1004-1020.

DOI: https://doi.org/10.30564/jasr.v3i2.1999

BILINGUAL PUBLISHING CO.
Pioneer of Global Academics Since 1984

Journal of Atmospheric Science Research
https://ojs.bilpublishing.com/index.php/jasr

ARTICLE

Planetary Layer Lapse Rate Comparison of Tropical, Montane and Hot Semi-Arid Climates of Nigeria

David O. Edokpa* **Precious N. Ede**

Department of Geography and Environmental Management, Rivers State University, Nigeria

ARTICLE INFO

Article history
Received: 15 June 2020
Accepted: 27 June 2020
Published Online: 30 June 2020

Keywords:
Lapse rates
Planetary layer
Climate belts
Nigeria, Emissions

ABSTRACT

This study assessed the pattern of planetary layer lapse rate across the major climate belts of Nigeria. Six years' data (2010-2015) for air temperature values between 1000 mbar and 850 mbar atmospheric pressure levels was acquired from Era-Interim Re-analysis data centre. The data was retrieved at 6-hourly synoptic hours: 00:00 Hr, 06:00 Hr. at 0.125° grid resolution. Results showed that the lower tropospheric layers throughout the various climate belts has a positive lapse rate. Findings also revealed that the average annual lapse rate condition were: Tropical wet zone (Port Harcourt) -5.6 °C/km; Bi-modal Tropical continental zone (Enugu) -5.8 °C/km; Montane zone (Jos) -6.5 °C/km; Mono-modal Tropical continental zone (Kano) -6.6 °C/km; and Hot semi-arid zone (Maiduguri) -6.6 °C/km. This average values presents the lapse rates to be near the Saturated Adiabatic Lapse Rate (SALR). Average diurnal results for the climate belts showed that lapse rate is higher during the afternoon and transition periods than the rest periods and increases from the coastal areas northward. The seasonal periods of highest lapse rates during the day time are from December - May (i.e. -5.8-9.5 °C/km) with slight decrease from June - November. The positive lapse rates of range -1.8 to 5.9 °C/km observed during the period of dawn across the entire region showed that infrared radiation was still being released and modified by less energetic mechanical turbulence that characterizes the surface layer across Nigeria. This also indicate that global warming is real and in substantial effect. The study findings imply that conditional instability prevailed over the entire region, therefore, the planetary layer environment will be of slow to moderate dispersive potential and will require forceful mechanism to lift emissions introduced into it. It is recommended that industrial stacks should be above 50 m to enhance the dispersion of emissions aloft.

1. Introduction

Lapse rate is the decrease of environmental air temperature in relation to vertical height. It is generated when the earth surface heated by solar radiation warms the overlaying air and the temperature of this surface ambient air reduces as it graduates upward from the source of warming i.e. earth surface [1]. The global average tropospheric lapse rate is -6.5 °C per km, however, this value varies with vertical height, latitude and season [2]. The lapse rate principle is based on a heated parcel of air that rises and expands due to decreasing pressure with

**Corresponding Author:*
David O. Edokpa,
Department of Geography and Environmental Management, Rivers State University, Nigeria;
Email: david.edokpa@ust.edu.ng; onojiede@gmail.co

 DOI: https://doi.org/10.30564/jasr.v3i2.2005

height. The air parcel's expansion reduces its temperature without exchanging heat with the surrounding environment. This is referred to as 'adiabatic lapse rate'. When dry air rises, it cools at the dry adiabatic lapse rate of -9.8 ^{o}C per km. This rate in the atmosphere depicts a scenario where there might be water vopour in the atmosphere but has no liquid moisture in form of fog, droplets or cloud [3]. When lapse rate reduces or increases with height, it is referred to as a 'positive' or 'negative' lapse rate respectively. The negative lapse rate also known as 'temperature inversion' occurs highly in the upper atmosphere (stratosphere). It also occurs within the planetary layer during the night when there is a reverse air temperature gradient. The decrease of environmental air temperature with altitude in the lower atmosphere (0-15 km) is very vital to the stability and dynamics of climatic variables that characterizes the lower atmosphere. The stability of air is boosted by its temperature distribution in the troposphere at different altitudes. Consequently, by observing the temperature variance at various heights between the surrounding environment and a rising air parcel, the stability conditions of the boundary layer atmosphere can be determined. Temperature stratification in the lower atmosphere is influenced majorly by these dynamics which includes dry and moist convection, heat exchanges, radiation flux, turbulence and wind shear. There is the balance of boundary layer climate through the effective altitudinal transmissions of heat and moisture. A sustainable mechanism that promotes the vertical displacement of an air parcel in the planetary layer is turbulence. Turbulence can either be thermal or mechanical and the latter is the dominant pattern across the planetary layer in Nigeria [4]. Vertical energy transfer in the troposphere is accomplished by the rate of turbulent motions and this enhances or reduces the energy exchange between the surface layer and lower atmosphere.

Various studies had shown that temperature decreases with altitude and that temperature lapse rate is one of the controlling factors governing the structure of any planetary atmosphere [5][6][1]. However, it has been explained [7] that studies on the vertical temperature structure of the lower tropospheric layer in many tropical locations of the earth, including areas where there are gaps in observational data, are completely insufficient. It was also admitted that the tropical region is principally characterized by more or less uniform decrease in temperature with height within the lower tropospheric layer. It was observed [8] that the use of constant and regular atmosphere measuring instruments like radiosonde and rocket in tropical locations is still at its poor state.

An estimation of tropospheric lapse rate [5] using the global monthly mean data of the NCEP/NCAP reanalysis (1948-2001) was conducted. The result showed that the average positive tropospheric lapse rate in the northern hemisphere as a whole and over the continents was between 6.1 to 6.2 ^{o}C/km. It was noted that at the sub-tropics, temperature decreases up to 20 km and at polar latitudes, temperature decreases up to 10 km. The seasonal and synoptic variations in near-surface air temperature lapse rate in south-central Idaho was examined using maximum temperature data from 14 synoptic stations [9]. The result showed that the average lapse rates from January to December ranged between -0.43 to -0.70 ^{o}C/100m. It was noted that lapse rate during humid conditions approximated the saturated adiabatic lapse rare (SALR) i.e. -0.4 to -0.5 ^{o}C/100m. Results also proposed that if observations are not available in the area of interest, then the environmental lapse rate (ELR) may be adequate for maximum air temperature computations.

Furthermore, [10] determined the mean moist and dry adiabatic lapse rates for the lower troposphere in the northern hemisphere for January and July. For January, average positive dry adiabatic lapse rate value was about 4.95 ^{o}C/km while in July it was 5.21 ^{o}C/km. Mean moist lapse rate was about 6.21 ^{o}C/km in January and about 5.10 ^{o}C/km in July. The mean annual lapse rate for both dry and moist conditions were 5.16 ^{o}C/km and 5.67 ^{o}C/km respectively. It was specified that a better choice for critical lapse rate would be a constant equal to 5.1 ^{o}C/km. Further emphasis revealed that hemispheric mean lapse rates in the mid and lower troposphere are within 0.4 ^{o}C/km of the moist adiabatic lapse rate in July. It was stated that the latitudinal distribution of tropospheric mean lapse rates clearly delineates two regimes in the atmosphere: a high latitude regime which exhibits the critical lapse rates and a low latitude regime where the lapse rates are principally moist adiabatic.

An assessment of the lapse rate values for China mainland by [6] showed that it generally has a branded distribution from southeast to northwest and range from -0.3 to -0.9 ^{o}C/100m in all seasons. On the plateau, the lapse rates range from -0.6 ^{o}C/100m in summer to -0.8^{o}C/100m in spring/winter. In northeast China, they are within -0.7 to -0.9^{o}C/100m. However, the stabilizing lapse rates value was around -0.6 to -0.8 ^{o}C/100m. Harlow et al., (2004) conducted an analysis of temperature lapse rate in the semi-arid south-eastern Arizona for one year. The result reveals that the lapse rate predicted from mean and maximum daily temperature data taken at 2m height was similar to the ELR i.e. -6 ^{o}C/km. The calculated values from radiosonde data were within -6 to -8 ^{o}C/km. Using 4 to 60 years' data, [11] estimated the mean positive lapse rate

DOI: https://doi.org/10.30564/jasr.v3i2.2005

(°C/100m) for the following regions such as US Rockies, Eastern North America, Northern South America, Scandinavia, Western Europe, Europe and Asia to be 0.58, 0.78, 0.61, 0.90, 0.62, 0.47 and 0.67 respectively.

It was mentioned that lapse rate is mostly steeper during day period than at night time as well as during hotter season than in colder periods [12]. It was also declared [13] that lapse rates are significantly controlled by synoptic airflow with shallower lapse rates associated with southerly air flows and northern flows associated with steeper lapse rates.

2. The Nigeria Climate Pattern

The study areas are situated in various climate belts of Nigeria. These are the tropical wet zone (Port Harcourt with coordinates: Longitudes 6° 57' - 7°59' E and Latitudes 4° 41' - 4°56' N); the bi-modal tropical continental zone (Enugu with coordinates: Longitude 07° 54' E and Latitude 06° 48' N); the montane climate (Jos with coordinates: 08° 53' E and Latitude 09° 51' N); the mono-modal tropical continental zone (Kano with coordinates: Longitudes 7° 47' - 9° 30' E and Latitudes 10° 32' - 12°24' N) and hot semi-arid zone (Maiduguri with coordinates: 13° 03' E to 13° 08' E and Latitude 11° 26' N to 11° 34' N). The Figure 1 shows the Nigeria climate belts and study areas.

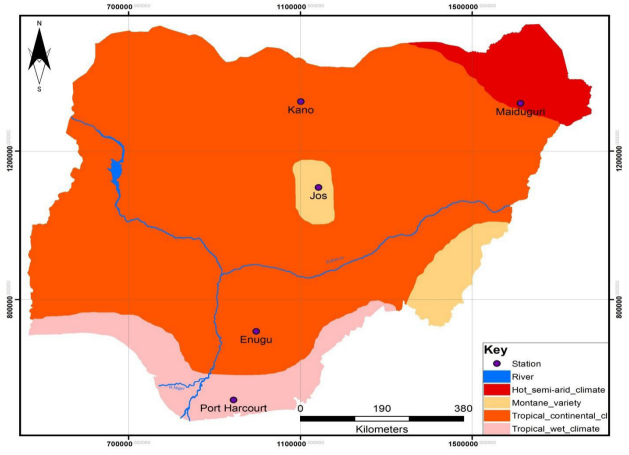

Figure 1. Climate Belts of Nigeria Showing Study Areas

Source: [4]

2.1 Tropical Wet Climate

This climate zone is found around the coastal areas, up to 150 km inland. This climate pattern is closely linked with the tropical monsoon climate influenced by the moisture laden air from the Atlantic Ocean. The weather producing system in the zone is the monsoon i.e. the south-westerly winds coming from across the Atlantic and blowing towards the thermal low-pressure system created by solar heating in the interior of the continent [14]. Average annual maximum temperature values vary between 27 °C to 32 °C most of the year. Average relative humidity in the zone range from 80 % with over 2400 mm of annual rainfall for places like Port Harcourt [15]. This climate belt (representative of the Niger Delta area) which is influenced by the humid and warm tropical maritime air mass (mT) almost throughout the year has the bi-modal rainfall regime. The rainfall is usually conventional in nature due to the region's closeness to the equatorial zone. The peak bi-modal rainfall period in July and September is dominant in the region.

2.2 Tropical Continental Climate

This climate belt is found inland, and covers over 80% of Nigeria's lower atmospheric domain [4]. It is demarcated by the bi-modal rainfall line (a moderate tropical continental type south of the line and an extreme mono-modal tropical continental type north of it). The southern end has subdued temperature ranges with higher annual bi-modal rainfall with a shorter dry season of about four months e.g. Enugu. The northern end has higher temperature ranges with lower annual mono-modal rainfall pattern but a longer dry season of six to eight months e.g. Kano. Rainfall decreases from the coastal southern part as one move towards the northern part of the line. It was disclosed that this northern end [15] is mostly influenced by the tropical continental air mass (cT) from across the Sahara Desert for most of the year. The climate zone has a wide range of relative humidity. Average annual rainfall and temperature vary from over 1700 mm and 26.3 °C in places like Enugu to below 800 mm and 26.1 °C in places like Kano respectively [4].

2.3 The Montane Variety Climate

This high altitude variety climate dominate on the Jos, Obudu, Adamawa and Mambilla plateaux. Air temperatures are very low both in the wet and dry seasons due to the highlands well over 1500 m above sea level [4][16]. The average temperature range all through the year in this zone is within 20 - 23 °C [4][17]. The mean annual rainfall in the areas such as the Mambilla plateau exceeds 1780 mm with peaks in June/July and September while dry season last between November and February [16].

2.4 Hot Semi-Arid Climate

The climate of the semi-arid zone in Nigeria is characteristically of the dry tropical type with distinct wet and dry seasons. The zone is found in the region of subtropical highs where subsiding air masses prevails [4]. The zone's position

DOI: https://doi.org/10.30564/jasr.v3i2.2005

in the continental interiors obstructs it of continuous influence of the tropical maritime air masses from the Atlantic Ocean. Hence, the cool and dry tropical continental air mass from the Sahara Desert dominates the region for most of the year. The average annual and diurnal range of air temperature is large and between 20 ^{o}C to 25 ^{o}C. Average minimum temperature range vary from 12 ^{o}C in December/ January to 23 ^{o}C in May. Average maximum temperature range from 31 ^{o}C in December/January to 40 ^{o}C in April. The warmest months are March and April when daytime temperature exceeds 40 ^{o}C [4]. According to [18], rainfall in the zone is highly variable and the onset of rain is erratic. The dry season is from October to early May, while the wet season is concentrated in a short period that runs from May to September [4][19]. The rainfall intensity is high between the months of July and August with peak in August and average range between 215 - 250 mm [4][14]. The rainfall peak in August is due to the presence of ITD which drives the maritime air mass across the zone. Typical average annual rainfall values range between 150 mm to less than 1000 mm [4][14][18]. It was stated that the zone is ravaged [20] with prolong increasing evapotranspiration, drought and desertification due to low rainfall amount. During the dry season, the atmosphere is strongly dominated by the dry dusty wind referred to as 'Harmattan' which transports dust over land from the Sahara Desert. Relative humidity is relatively low throughout the year ranging between 18 - 63 % with low and high peaks during the dry and wet seasons respectively. Due to the massive landmass void of much vegetation to retard wind velocity, average amount range from 1.5 - 12 m/s with average annual sunshine duration ranging between 8 - 11 hours [4].

3. Methodology

The data for this study was sourced from the Era-Interim Re-analysis platform for the period of six years (2010-2015). The data was acquired for 6-hourly interval at 0000, 0600, 1200 and 1800 synoptic hours. According to [14], meteorological observations are made at fixed observing hours. The main synoptic hours internationally agreed upon are 00:00 (midnight), 06:00 (6am), 12:00 (noon) and 18:00 (6pm) Greenwich Mean Time. Upper air temperature values at pressure level 850 mbar and 1000 mbar for an approximate surface level was obtained. The Era-Interim Reanalysis data is the newest universal atmospheric data generated by the European Centre for Medium-Range Weather Forecast. The gridded products comprise a large variety of data for surface and upper air. Furthermore, its application has surpassed expectations and speaks volume about the outstanding successes obtained in recent years [4]. It was highlighted that the Era-Interim Global data provides meteorological parameters the required understanding for enhanced knowledge of the circulatory system across West Africa [21]. The Era-Interim data for the specified years was obtained at 0.125^{o} spatial resolution. This low resolution was chosen to obtain a reliable spatial scale across study areas.

The vertical temperature profile for the lower atmosphere is given by:

$$T(z) = T_0 - \Gamma.z \qquad \text{equation 1}$$

Where Tz and T_0 are temperature at the varying heights, Γ is the environmental lapse rate at 6.5 ^{o}C/km and z represents any vertical height. An important aspect of environmental air temperature is that it decreases with height above the surface within the troposphere up to 15km. The rate of decline is defined by:

$$\Gamma = -\frac{\partial T}{\partial z} \qquad \text{equation 2}$$

The environmental lapse rate for the area was determined using the following equation [22].

$$\Gamma = \frac{T_{850mbar} - T_{1000mbar}}{\partial z} \qquad \text{equation 3}$$

Where:

$T_{850mbar}$ = air temperature at reference height (between 1-1.4 km)

$T_{1000mbar}$ = air temperature at surface level (approximately 0.01 km)

∂z = the difference in elevation between the two heights.

The relationship between the ELR and the air parcel lapse rates i.e. dry and moist adiabatic lapse rates (DALR & MALR) was used in this study to determine the major domain of the atmospheric stability conditions as it relate to the average lapse rate pattern of the study region. The following criteria were adopted for stability classification [4,23].

(1) ELR =-6.5 ^{o}C/km
(2) DALR =-9.8 ^{o}C/km
(3) SALR =-5.0 ^{o}C/km

When:

(1) ELR < SALR < DALR = Stable Atmospheric Conditions

(2) SALR < DALR < ELR = Unstable Atmospheric Conditions

(3) SALR < ELR < DALR = Conditional Instability

(4) ELR =DALR = Neutral Atmospheric Conditions (Unsaturated Air)

(5) ELR= SALR = Neutral Atmospheric Conditions (Saturated Air)

DOI: https://doi.org/10.30564/jasr.v3i2.2005

MATLAB software was used in resolving the mathematical procedures and the occurrence of lapse rate distribution.

4. Results

The Figures 2 - 7 presents the average diurnal, seasonal and annual lapse rate trend for the study areas during the specified synoptic hours (00:00 Hr; 06:00 Hr; 12:00 Hr and 18:00 Hr). From the study, it is shown that the lower tropospheric layers throughout the various climate belts has a positive lapse rate. Results showed that the average annual lapse rate condition for the climate belts in Nigeria are: Tropical wet zone (Port Harcourt) -5.6 ^{o}C/km; Bi-modal Tropical continental zone (Enugu) 5.8 ^{o}C/km; Montane zone (Jos) -6.5 ^{o}C/km; Mono-modal Tropical continental zone (Kano) -6.6 ^{o}C/km; and Hot semi-arid zone (Maiduguri) -6.6 ^{o}C/km (Figure 2). This shows that lapse rate increased from the coastal area of Port Harcourt towards the semi-arid interiors of Maiduguri. The average annual lapse rate indicated that Jos, Kano and Maiduguri followed the standard environmental lapse rate (ELR) of -6.5 ^{o}C/km while Port Harcourt and Enugu followed the moist or saturated adiabatic lapse rate pattern. However, the average annual lapse rate for the entire region is in the moist adiabatic range. The position of Nigeria is principally within the lowland moist tropics north of the equator and branded by a high temperature system [4]. It was noted that Nigeria's latitudinal position within the tropics and the mostly low relief enhances the high-temperature all the year round [24]. The high surface temperature creates a dynamic system where energy fluxes are transferred from the surface to the upper layers of the troposphere [4].

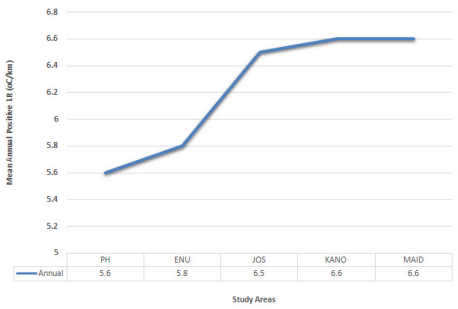

Figure 2. Mean Annual Lapse Rate Pattern for the Study Areas

Average diurnal results for the climate belts showed that lapse rate is steep during the afternoon and transition periods (i.e. 12:00 and 18:00 hours) for the entire areas than the rest periods (Figure 3). There is an average increase of -6.3 ^{o}C/km in the coastal wet zone to -9.0 ^{o}C/km respectively in the hot semi-arid areas of Nigeria. The Figure 6 shows that the seasonal period of March - May (MAM) for Kano and Maiduguri during the afternoon period had a positive lapse rate value of 9.5 ^{o}C/km and 9.4 ^{o}C/km respectively. These values are close to the dry adiabatic lapse rate of 9.8 ^{o}C/km and this indicate the very dry nature of the lower atmosphere within these climate belts. It is noted that MAM is the hottest period in the climate zones as air temperature exceeds 40 ^{o}C. The higher positive values (7.1 and 8.1 ^{o}C/km) noted at the southern bi-modal tip of Nigeria's Port Harcourt and Enugu in January indicate the period of peak dry season in the areas where the dry north-easterly wind covers the areas, pushing back the moist south-westerly wind over the Atlantic Ocean.

The early hours of the day (00:00-06:00 hours) exhibited a lower average positive lapse rate across the entire region, however, while there was a near uniform trend at 00:00 hour of range -5.1 to -5.9 ^{o}C/km, there were variations during the 06:00 hour of range -3.5 to -5.1 ^{o}C/km (Figure 3). The lower lapse rate trend of -3.5 ^{o}C/km (Figure 3) at the continental interiors during the period of dawn (06:00 hour) indicate the large diurnal temperature difference that is prominent in the areas due to the dryer air than at the coastal zone with moist air. The average seasonal values for the periods of dawn exhibited a positive lapse rate of range 4.4 - 6.2 ^{o}C/km and 1.8 - 5.4 ^{o}C/km across the entire region for 00:00 and 06:00 hours respectively (Figures 4 and 5). The lower values observed at 06:00 hour across the entire region portrays the much released longwave radiation that took place between the hours.

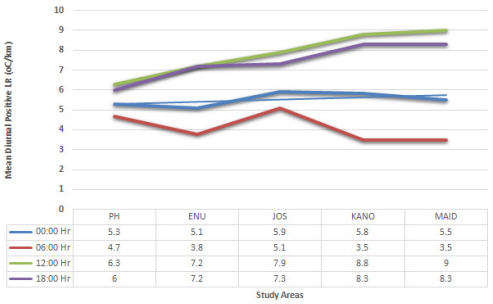

Figure 3. Mean Diurnal Lapse Rate Pattern for the Study Areas

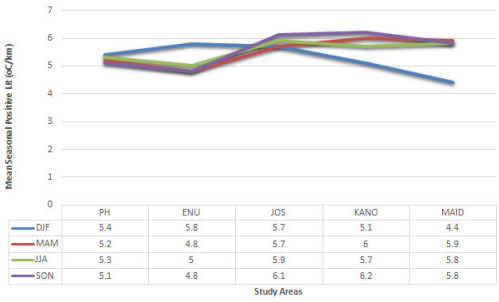

Figure 4. Mean Seasonal Lapse Rate Pattern for the Study Areas (00:00 Hour)

DOI: https://doi.org/10.30564/jasr.v3i2.2005

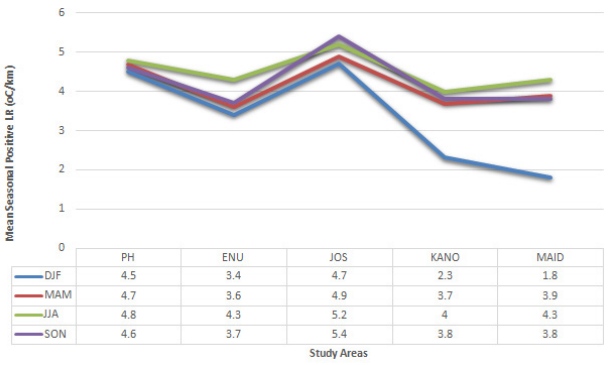

	PH	ENU	JOS	KANO	MAID
DJF	4.5	3.4	4.7	2.3	1.8
MAM	4.7	3.6	4.9	3.7	3.9
JJA	4.8	4.3	5.2	4	4.3
SON	4.6	3.7	5.4	3.8	3.8

Figure 5. Mean Seasonal Lapse Rate Pattern for the Study Areas (06:00 Hour)

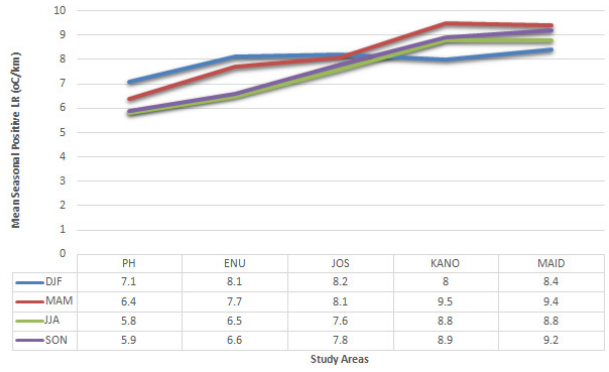

	PH	ENU	JOS	KANO	MAID
DJF	7.1	8.1	8.2	8	8.4
MAM	6.4	7.7	8.1	9.5	9.4
JJA	5.8	6.5	7.6	8.8	8.8
SON	5.9	6.6	7.8	8.9	9.2

Figure 6. Mean Seasonal Lapse Rate Pattern for the Study Areas (12:00 Hour)

The positive lapse rates observed during the night and dawn across the entire region showed that infrared radiation was still being released even during the periods of dawn. Solar insolation peaks at noon because at that time incoming solar radiation exceeds heat loss from the earth's surface. Therefore, surface temperature is still increasing. Maximum temperature occurs when the rate of heat loss from the earth's surface is the same as rate of heat gained from solar insolation. This occurs later in the afternoon usually (14:00-16:00 hours). At 18:00 hour, infrared exceeds insolation and this can continue till the periods of dawn [4].

Also, the effect of greenhouse gases build-up such as increased carbon dioxide (CO_2) concentration in the atmosphere and the essence of global warming enhance the occurrence of positive lapse rates during the dawn. This is due to the heat exchanges that takes place between the earth surface and lower atmosphere i.e. 'the surface energy releases and the atmospheres energy returns'. This creates a mechanism whereby an upward heat transfer still occurs across the boundary layers that maintains the specified lapse rates. The notable factors that also enhance positive lapse rate values during the period includes the availability of less energetic surface mechanical turbulence at night across Nigeria [4], the heat capacity of the surfaces and the energy stored at the surfaces.

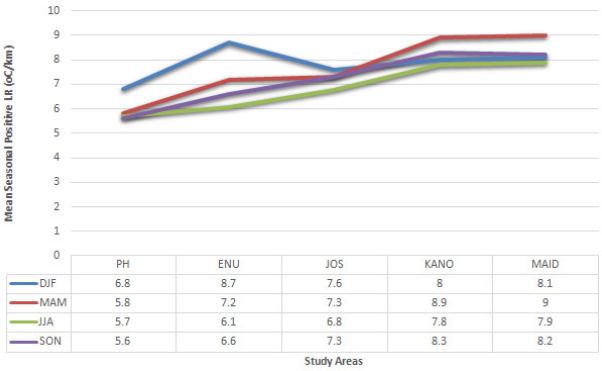

	PH	ENU	JOS	KANO	MAID
DJF	6.8	8.7	7.6	8	8.1
MAM	5.8	7.2	7.3	8.9	9
JJA	5.7	6.1	6.8	7.8	7.9
SON	5.6	6.6	7.3	8.3	8.2

Figure 7. Mean Seasonal Lapse Rate Pattern for the Study Areas (18:00 Hour)

5. Discussion

The lapse rate is a vital factor that impacts the atmospheric stability conditions of any area. It affects the stability of air masse across the lower troposphere through the relationships between the ELR, DALR and the SALR.

According to [25], there are two aspects of instability, i.e. absolute instability (where ELR is higher than both the DALR and SALR) and the conditional instability (where the ELR is within the range of the SALR i.e. -1 to -6.5 ^{o}C/km but lower than the DALR i.e. -9.8 ^{o}C/km). A significant extract of lapse rate analysis is the conditional instability arrangement of the lower troposphere. The term 'conditional' is utilised since air is required to be pushed aloft before it gets to a point where free ascent takes over. The lapse rate is the only source to determine this aspect of atmospheric stability. This study showed that the average lapse rate values for the entire region is close to the ELR and the SALR and lesser than the DALR. During this conditions, stable air is forced to rise to certain height where condensation occur, and, on releasing latent heat continues ascension freely. It should be noted that the ELR represents an average condition where heating, mixing and wet adiabatic process are also taking place [3]. The relationship between the ELR and the DALR regulate the stability of air and the rate with which emissions will be dispersed and diluted in the atmosphere. When the ELR is the same as the DALR, neutral condition exists in the atmosphere. It was disclosed that the ELR [9] is exclusively relevant to maximum temperature as it commonly overestimates minimum temperature and mean temperature lapse rates. From the lapse rate analysis, conditional instability exists across the lower troposphere of the study areas. This stability condition implies that a force is required to lift emissions dispersed at ground level either by

DOI: https://doi.org/10.30564/jasr.v3i2.2005

mechanical or thermal turbulence. Mechanical turbulence dominates the surface layer of Nigeria (10-50 m), while thermal turbulence is prominent aloft [4]. This means that ground level emission sources will require moderate to stronger wind velocity to lift pollutants to a height where further transportation and dispersion is effected by thermal turbulence. Where mechanical turbulence is weak at the surface layer, stacks for stationary emission sources must be above 50 m in any location in Nigeria to have a better dispersion rate.

6. Conclusion

This study has analysed the lapse rate pattern of major climate belts across Nigeria. The lapse rate which is the variation or change in air temperature with vertical height in the troposphere significantly influence how released emissions are conveyed and diluted in the lower atmosphere. Findings from this study revealed that positive lapse rate conditions exist throughout the entire region within the periods of study. Results showed that the average annual lapse rate for boundary layer conditions in Nigeria is within the environmental/moist positive adiabatic lapse rate range (i.e. -5.6 to -6.6 ^{o}C/km) thereby allowing a state of conditional instability to persist. In this atmospheric condition, an air parcel will be forced to rise by either mechanical or thermal turbulence at any given time or location under a stable atmospheric state. Findings from this study also showed that lapse rate is higher and increases from the coastal areas to the northern fringes of Nigeria most especially during the day and lower during the periods of dawn. The positive lapse rate indicated during periods of dawn emphasises the continuousl release of infrared radiation from the ground surface as well as the reality of global warming due to the build-up of greenhouse gases in the atmosphere.

References

[1] Kattel, D.B., Yao, T., Yang, W., Gao, Y., Tian, L.. Comparison of temperature lapse rates from northern to southern slopes of the Himalayas. Int. J. Climatol., 2015, 35, 4431-4443.
DOI: 10.1002/joc.4297

[2] Hartmann, D. L.. Global Physical Climatology. New York: Academic Press,1994.

[3] Hemond, H. F., Fechner, E. J.. Chemical Fate and Transport in the Environment (3rd Edition). Academic Press, 2015. Available from:
https://www.sciencedirect.com/topics/earth-and-planetary-sciences/adiabatic-lapse-rate

[4] Edokpa, O.D.. Atmospheric Stability Conditions of the Lower Atmosphere in Selected Cities in Nigeria. An Unpublished Ph.D. Thesis, Department of Geography and Environmental Management, University of Port Harcourt, Nigeria,2018.

[5] Mokhov, I. I., Akperov, M. G.. Tropospheric Lapse Rate and its Relations to Surface Temperature from Reanalysis Data. Atmospheric and Oceanic Physics, 2006, 42(4): 430-438. ISSN 0001-4338, lz vestiya.

[6] Li, X., Wang, L., Chen, D., Yang, K., Xue, B., Sun, L.. Near-surface air temperature lapse rates in the mainland China during 1962-2011. J. Geophys. Res. Atmos., 2013, 118: 7505-7515.
DOI: 10.1002/jgrd.50553

[7] Olajire, M. A., Mattew, O. J.. Determination of the vertical variations in temperature and longwave radiation within the grey Earth's troposphere using radiative equilibrium profile model. International Journal of Physical Sciences, 2013, 8(36): 1800-1806.
DOI: 10.5897/IJSP2013.3975

[8] Roger, G. B., Richard, J.C.. Atmosphere, Weather and Climate. New York: Rutledge,1995.

[9] Blandford, T. R., Humes, K. S., Harshburger, B. J., Moore, B. C., Walden, V. P., Ye, H.. Seasonal and Synoptic Variations in Near-surface Air Temperature Lapse Rate in a Mountainous Basin.Journal of Applied Meteorology and Climatology, 2008, 47: 241-261.
DOI: 10.1175/2007JAMC1565.1

[10] Stone, P. H., Carlson, J. H.. Atmospheric Lapse Rate Regimes and their Parameterization. Department of Meteorology, Massachusetts Institute of Technology, Cambridge 02139. 1979, 36: 415-423.

[11] Diaz, H. F., Bradley, R. S.. Temperature Variations during the Last Century at High Elevation Sites. Climate Change, 1997, 36: 253-279.

[12] Roland, C.. Spatial and seasonal variations of air temperature lapse rates in alpine regions. J. Climate, 2003, 16: 1032-1046.

[13] Holden, J., Rose, R.. Temperature and surface lapse rate change: a study of the UK's largest upland instrumental record. International Journal of Climatology, 2011, 31(6): 907-919.
DOI: 10.1002/joc.2136

[14] Ayoade, J. O.. Introduction to Climatology for the Tropics (2nd Edition). Ibadan: Spectrum Books, 2004.

[15] Oluyole, K. A., Emeka, L. A., Aigbekaen, E. O., Oduwole, O. O.. Overview of the Trend of Climate Change and its Effects on Cocoa Production in Nigeria. World Journal of Agricultural Research, 2013, 1(1): 10-13.
DOI:10.12691/wjar-1-1-3

 DOI: https://doi.org/10.30564/jasr.v3i2.2005

[16] Borokini, T. I., Babalola, F. D., Amusa, T. O., Ivande, S. T., Wala, Z. J., Jegede, O. O., Tanko, D., Ihuma, J.O.. Tropical Montane Forest Biodiversity in Nigeria - Case Study of NgelNyaki Forest Reserve, Mambilla Plateau. International Journal of Environmental Science, 2012, 1(2): 95-104.

[17] Sowunmi, F. A., Akintola, J. O.. Effects of Climate Variability on Maize Production in Nigeria. Research Journal of Environmental and Earth Sciences, 2010, 2(1): 19-30.

[18] Fabeku, B.B., Okogbue, E.C.. Trends in Vegetation Response to Drought in Sudano-Sahelian Part of Northern Nigeria. Atmospheric and Climate Sciences, 2014, 4: 569-588.

[19] Agunbiade, O., Adelekan, I.. Monitoring Drought Occurrences over the Sahel and Sudan Savannah of Nigeria using NDVI. International Journal for Research in Applied Sciences & Engineering Technology, 2017, 5(v): 2178-2188.

[20] Odjugo, P., Ikhuoria, A.. The impact of climate change and anthropogenic factors in desertification in the semi-arid region of Nigeria. Global Journal of Environmental Science, 2003, 2(2): 118-126.

[21] Okonkwo, C., Demoz, B., Tesfai, S.. Characterization of West African Jet Streams and their Association to ENSO Events and Rainfall in ERA-Interim 1979-2011. Advances in Meteorology, 2014, 1-12.

[22] Harlow, R. C., Burke, E. J., Scott, R. L., Shuttleworth, W. J., Brown, C. M., Petti, J. R.. Derivation of temperature lapse rates in semi-arid south-eastern Arizona. Hydrology and Earth System Sciences, 2004, 8(6): 1179-1185.

[23] Weli, V.E., Edokpa, O.D.. Analysis of Lower Tropospheric Lapse Rate Trend over Port Harcourt Coastal City, Nigeria. Atmospheric and Climate Sciences, 2018, 8: 134-142.

[24] Ulor, C. O.. Assessment of Rainfall Shifts in Qwerri, Nigeria,2012. Available from: http://emekahouse.blogspot.com.ng/search/label/Rainfall%20Trend%201996-2005

[25] Talkbloke. Lapse rate and atmospheric stability, 2012. Available from: https://tallbloke.wordpress.com/2012/01/31/back-to-basics-2-lapse-rates-andatmospheric stability/

DOI: https://doi.org/10.30564/jasr.v3i2.2005

BILINGUAL PUBLISHING CO.
Pioneer of Global Academics Since 1984

Journal of Atmospheric Science Research
https://ojs.bilpublishing.com/index.php/jasr

ARTICLE

Understanding the Nexus between Climate Change, the Shift in Land Use toward Cashew Production and Rural Food Security in Ghana; the Experiences of Farmers in the Transition Zone of Ghana

Victor Adjei[1*] Moses Ackah Anlimachie[2] Eunice Elorm Ativi[3]

1. Climate Change and Sustainable Development, University of Ghana, Legon, Accra, Ghana
2. Educational Futures, University of South Australia, Adelaide, Australia
3. Faculty of Veterinary and Food Safety, Eduardo Mondlane University, Mozambique

ARTICLE INFO

Article history
Received: 17 June 2020
Accepted: 27 June 2020
Published Online: 30 June 2020

Keywords:
Rural Ghana
Climate variability
Farmland use
Small-holding farmers
Food security
Women venerability

ABSTRACT

This study summarises the findings from a study investigating rural small-holding farmers' experiences on the shift from food crop to cashew in the forest/savanna transitional agro-ecological zone of Ghana and its impact on rural food security. Using a mix method approach, the study sampled the views of 400 farmers from 9 farming communities in the Wenchi Municipality of Ghana via questionnaire and semi-structured interview and collated statistical data on crop production to trace the nexus between climate change, agrarian land-use decisions and food security. The study found evidence of increasing shift from food crop to cashew production. This was evidenced by increasing cashew cultivation and cashew output and decreasing total land acreage for food crops and increasing food insecurity of farmers. The findings revealed that about 71% of farmers had expanded their cashew farms and another 41.0% have turned their food crops' lands to cashew production. Besides cashew production, (57.0%) has overtaken the traditional food crop -maize (25.5%) production in terms of output. Instructively, the study found that the main motivation for the shift from food crop to cashew production is not only to maximise income in bulk, but also climate change adaptability issues. The study found that the cashew crop is resilient in adapting to the changing climate and less prone to pests' invasion compared to maize in the study District. The study found that food security among rural folks had been seriously compromised by the conversion of farmlands from food crop to cashew farming. Although, the study found that female farmers have higher consciousness to food security yet less motivated to shift from food crop to cashew crop production compared to men. Worryingly, females are the hardest hit group because of their low ownership of or access to farmlands and low voices of women in farmland use decision making in a men-dominant rural extended family setting of the study District. The study concludes that climate change adaptability concern has introduced a new set of risks including crop failure due to changing rainfall pattern and increasing incidence of pest invasions forcing the rural folks to compromise innovative indigenous farming focus and practices that have helped them to navigate extreme food poverty. This study, therefore, argues for improved food crop seeds tailored to the specific climatic context and innovative farming practices that beef-up small-holding farmers' capacity to navigate climate change to continually produce food crop to ensure rural food security and sustainability.

**Corresponding Author:*
Victor Adjei,
Climate Change and Sustainable Development, University of Ghana, Legon, Accra, Ghana;
Email: victoradjei73@gmail.com

 DOI: https://doi.org/10.30564/jasr.v3i2.2010

1. Background

Agriculture is the main 'life support' for broad-based economic growth, poverty alleviation and food security in Sub-Saharan Africa (SSA), having economic and social impacts. Undeniably, incomes accrued from agriculture in the sub-region (SSA) are much more effective in reducing poverty than Gross Domestic Product (GDP) growth in other sectors [1].

Agriculture remains the heartbeat of the economy of most of the third world countries employing more than half of the populace and contributing immensely in GDP. In Ghana, agriculture employs half of the labour force [2]. About 70% of farmers in Ghana engaged in crop production [3]. Livestock, cocoa, fish and forest products dominate Ghana's agricultural sector while non-traditional exports such as mango, pineapple, cashew nuts are progressively becoming very viable to the economy of Ghana [4].

Agriculture in Ghana is rural, dominated by small-holder farmers [5]. About 52% of the Ghanaian rural workforce are into small-scale agriculture, accounting for about 80% of the agriculture produce and 20% of the GDP [5,6]. However, smallholding farmers are less productive and are among the poorest in Ghana, accounting for about 80% of the poverty incidence. This is because agriculture productivity is low as it is rain-dependent, small-scaled and less mechanised. More worriedly, in recent times, agricultures in Ghana has come under the rampaging effects of climate change evident in intensified long dry seasons, erratic rainfall patterns, excessive evaporation and the drying of freshwater bodies, increasing incidence of pests' invasion, particularly on cereal crops. The effects of these have resulted in the increasing incidence of crop failures, low productivity, increasing food insecurity, which is putting about 46% of Ghanaians [whose livelihood is dependent on small-holding agriculture] at risk. Even more so is the fact that only 300 km^2 of the 41000km^2 arable under cultivation is irrigated in Ghana, thus making agriculture highly exposed to climate variability [7,5]. The combined effect of these is that in the study Municipality, farmers attempt to navigate the impact of climate change on the increasing incidence of food crop failure arising from erratic rainfall pattern, increasing dryness and pest invasion, farmers are rapidly shifting land use from food crop to cash crop, particular cashew nut production.

As a tropical crop, cashew (Anacardium occidentale L.) is presently grown around the equator, globally. Even though cashew was introduced in West Africa in the middle of the 16th century [8], the acceptance of cashew as cash crop began in the 1950s and has only become an intensively grown cash crop since 1990s. Currently, West Africa is among areas dominated in producing cashew accounting for 45% of the worldwide production in 2015 [9]. In Ghana, cashew as a non-traditional export crop began to receive attention in the late 80s. The export of Raw Cashew Nuts (RCNs) increased appreciably from 15 metric tonnes to 61,590 metric tonnes between 1990 and 2008, the annual production was estimated to be 26,452 metric tonnes [4]. Cashew is grown in three agro-ecological zones in Ghana, namely in the Interior Savanna (Guinea Sudan Savanna), Forest-Savanna Transitional and, the Coastal Zone [4]. However, among these three zones, the middle belt (Forest-Savanna Zone) is best suitable for cashew production in Ghana [4,10]. It is estimated that Ghana has about 3 million hectares (ha) of arable land suitable for the cultivation of cashew farm, however these arable lands in the three aforementioned ecological zones, especially the Savanna-Forest Transition Zone is the main food basket of Ghana, hence the more expansion of cashew farms is tantamount to decreasing farmland for food crop production [4]. This study, therefore, seek the answer to the following questions:

(1) To what extents are farmers shifting land use from food crop to cashew production in the Transition Zone of Ghana?

(2) What factors and motivation underpinned farmers' shift of land use from food crop to cashew production?

(3) What is the effect of the shift of land use from food crop to cashew production on rural food security?

The research, therefore, seeks an understanding of the seemingly growing shift of land use from food crop to cashew production in the Forest/Savanna Transitional Agro-ecological Zone of Ghana and its implication for rural food security and sustainability. The study tracked the nexus among climate change, farmers adaptability to climate change and rural food security to inform a more detailed study on innovative practices that can fortify rural livelihoods and food security.

2. Methodology

2.1 The Study Sites

The study was conducted in the Wenchi Municipality in the Bono Region (formerly Brong Ahafo Region) of Ghana. The district was randomly selected from a list of districts[1] that fall within the Transitional Zone of Ghana. The region is the major cashew production area and is located in the Forest/Savanna Transition agro-ecological Zone

[1] *Ghana has a-3 tier governance structures of national, regional and district levels. There are 16 regions and 254 districts. The Ministry of Education classifies districts into educationally deprived and non-deprived base on access and quality outcomes indicators. Seventy-five (75) district were classified as educationally deprived in 2015, these are also the rural-dominated district*

DOI: https://doi.org/10.30564/jasr.v3i2.2010

with a population of 89,739 [11]. The study Municipality occupies 7,619.7 square kilometres with 180 communities of which 70% of the local communities (villages and towns) are rural [12]. In Ghana, communities with a population of less than five thousand (5000) people are defined as rural areas [6]. The Municipality rurality is characterised by small-holding farming. The imprint of the agrarian land used in the Municipality is evident in her settlement pattern characterised by several smaller rural communities scattered across the district [13]. The study area lies between latitude 7°27N and 8°30N and longitudes 1°30W and 2°36W. The economy of the Municipality is driven by agriculture and its related activities. The sector accounts for 65.2% (33,817) of the active labour force compared with 57.0% at the nationwide level [2]. The study area has a bimodal rainfall pattern with peaks in June/July as well as September/October with a marked dry season from November-March. Average annual rainfall and temperature are 800-1200mm and 26^{0}C respectively [14].

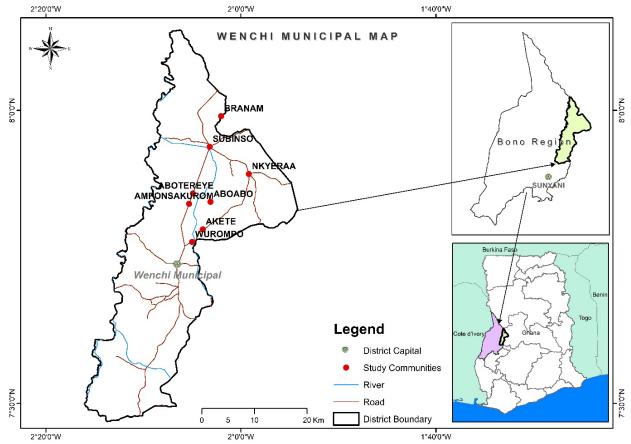

Figure 1. Map of Wenchi Municipality showing the study area

2.2 Participants and Data Collection and Methods

The study uses mix-method research by triangulating qualitative and quantitative methods and primary and secondary sources of data. Quantitatively, the study used surveyed method to sample the views of small-holding farmers. The study combined cluster cross-sectional and simple random sampling methods to select 400 small-holding farmers across nine (9) communities, including *Abotareye (55), Aboabo (30), Subenso No 1 (70), Subenso No 2 (40), Akefe (15), Nkyeraa (45), Brenam (55), Wurampo (20), and Amponsakrom (70)* to participate in this study via the administration of close-ended questionnaires. The questionnaire elicited a rage of farmers responses on climate (temperature and rainfall), farming activities, farmers' association, income accrued from cashew, demographic information and so on. The component of the respondents comprises both male and female farmers. Additionally, statistical secondary data on farm acreage, crop outputs and pesticides use were also collated from the Agricultural Department Office of the study Municipality. The quantitative data (questionnaires and secondary statistical data) were quantitatively analysed with SPSS and the results displayed in table and charts.

Also, in-depth semi-structured interviews were conducted with 6 key farmer-informants, probing farmers' motivation and experiences regarding cashew and food crop production, and food security. The discussions were audio-recorded with the permission from participants and, the data were later transcribed and thematically analysed to embellish the statistical result from the analysed responses from the questionnaires and the secondary data from the Municipal Department of Agricultural. Analytical summaries of the interview were developed to assist in the identification of the overarching themes for the study. In all, seven field workers were engaged.

3. Results and Discussion

Socio-economic characteristics of cashew farmers sampled are shown in Table 1. Majority of the cashew farmers were males (87.2%) whereas very few were females (12.8%). Greater number of the respondents were between the ages of 36-59 years (54.0%) while few of them were above the age of 60 years (10.8%). About 35.3% of the sampled cashew farmers were below the age of 35 years. About a third of the population of Wenchi comprises settlers [migrant farmers] form the five northern regions of Ghana making the Municipality multi-ethnic [2]. The indigenes who happened to be the Bono's were 41.5%. On education, it was revealed that the greater part of the respondents had not received formal education (29.8%). From Table 1, 26.5% were junior/middle school leavers whereas 18.3% of the farmers had received second cycle education. About 28% of the farmers were either primary or tertiary school graduates (see Table 1). However, about gender disparity, male farmers were better educated than their female counterparts. The results of the present study corroborate a study by [15] that education level of male farmers supersedes female farmers in the Nkoranza South Municipality. Approximately 43% of the female respondents had not received formal education as against 27.8% of male farmers. Moreover, with junior high/middle school, the percentage of male farmers (26.4%) and female (27.5%) were almost at par. Better still, the percentage of senior high graduates among male respondents (19.2%) was higher than the female respondents (11.8%). On tertiary education, the male farmers (14.0%) were

 DOI: https://doi.org/10.30564/jasr.v3i2.2010

better educated than their female cashew farmers (3.9%). A study by [16] revealed that the education attainment of a farmer has a major consequence on the farmer's productivity. It was observed that a higher percentage of the respondents had a family size around 1-5 (46.0%). The result of the study showed that the average household size is around 6-10 (42.5%) with about 2.3% of households having more than 10 members. The results also show that about 66 % of the farmers owned farmland with the rest patterning with or working for landlord/ladies on *adonkye (farm and let's share)*. More men than women own farmland in the Municipality. Farmers' background point to low educational attainment which was found to be the factor for the low productivity as found by [17] and [13].

Table 1. Socio-characteristics of farmers (participants)

Characteristics	Frequency	Percentage
Gender		
Male	349	87.2
Female	51	12.8
Total	400	100
Age		
≤ 35	141	35.3
36-59	216	54.0
≥60	43	10.8
Total	400	100
Tribe		
Bono	166	41.5
Mo	25	6.3
Settler from the north	198	49.5
Others	10	2.5
Total	400	100
Education		
No formal education	119	29.8
Primary	51	12.8
Junior High Sch./Middle School	106	26.5
Senior High Sch./O'level	73	18.3
Tertiary	51	12.8
Total	400	100
Literacy		
Cannot read and write	188	47.0
Can read only	19	4.8
Can write only	3	0.3
Can read and write	192	48.0
Total	400	100
Household size		
1-5	184	46.0
6-10	170	42.5
> 11	9	2.3
Total	400	100
Farmer identification		
Landlord/lady	264	66.0
Partner farmer	52	13.0
Resident farmer	83	20.8
N/A	1	0.3
Total	400	100
Acquisition of land		
Family land	107	26.6
Personal land	162	40.5
Rented land	94	23.5
Purchased	37	9.3
Total	400	100
Part of cashew sold		
Nut	400	100
Fruit	0	0

3.1 Characteristics of Cashew Farming in Wenchi Municipality

One dominant farming activity was the usage of weedicides/herbicides (88.0%) to clear weeds instead of the normal cutlass weeding. Pruning (89.5) too was pervasive unlike fungicides/spraying (16.5%) and ploughing (23.5%). The study found that (informant interview) using herbicides to '*burn*' weeds was much economical than employing a labourer to use a cutlass. Others too did not have much problem with weeding because such farmers normally used the land to cultivate food crop (93.3%) to check weeds unless it was the off-farm season. Historical records on pesticides application at the Municipal Agricultural Office as captured in Figure 1 indicates an increasing used in pesticides, especially, among farmers who cultivate maize due to the increasing incidence of pest invasion in recent times.

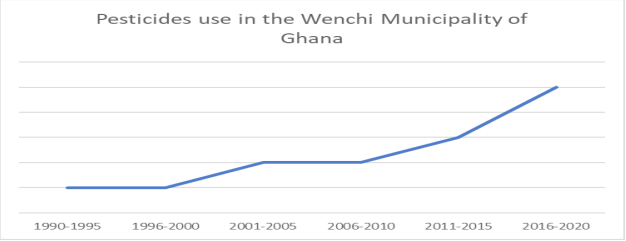

Regarding farming methods, the results revealed that the majority (93.3%) of the framers intercropped cashew with other crops, but at the infant stages of the cashew crop. However, the opportunity for intercropping reduces as the cashew crop matures. The result resonates with a study by [11] that most of the cashew farmers practice intercropping but when the cashew trees start forming canopies over time, it makes mixed cropping difficult to practice. Very few respondents practised monoculture (6.8%). Two paramount reasons were assigned to this intercropping farming system (informants). One was to en-

DOI: https://doi.org/10.30564/jasr.v3i2.2010

sure continual food supply to the household and the other one too to control weeds. The study also showed that the farm size of most of the respondents (67.0%) was 2 hectares whereas farmers with farmlands greater than 2 hectares were 33.0%. The study agrees with a study by [18] that cashew in Ghana is grown as a smallholder crop and the commercial plantations sector is very small. According to the paper, the majority of cashew farms are owned by smallholders, with farms ranging in size from a minimum 0.8ha (2 acres) to 3.0 ha (5 acres). The average price for a new land per hectare was around GHS120.00 (US$21) as of 2019-2020 farming season. The average cost of production in the study area was approximately GHS 2,205 per hectare (i.e. GHS 900 per acre). On acquisition of cashew farmlands, about half (49.8%) of the respondents farmed on their lands while 26.8% had their cashew on family lands. Others too (23.5%) farmed on rented lands in the Municipality.

The data from the Department of Agriculture in the Municipality clearly showed that between the year 2013 and 2017, there had been appreciable percentage increase in area under cultivation (36%), production (285%) and production per yield (183%). The average percentage increase for the five years under review was 7.2%, 57% and 37% respectively. This exponential increase in production from 2013 to 2017 was driven by the profit (53.4%) accrued from cashew business and probably vulnerability of food crops to climate change (10.8%).

Table 2. Estimated production figures for cashew from 2013-2017 in Wenchi Municipality

DEPARTMENT OF AGRICULTURE, WENCH MUNICIPALITY					
CURRENT ESTIMATED PRODUCTION FIGURES FOR CASHEW					
Crop	Cashew				
Year	2013	2014	2015	2016	2017
Area under cultivation (ha)	7,980.00	8,424.20	8,867.60	9,852.80	10,838.80
Production (yield /ha)	0.6 mt/ha	0.8 mt/ ha	0.89 mt/ ha	1.6 mt/ha	1.7 mt/ha
Production	4788.48 mt	8739.4 mt	7094.1 mt	15764.5 mt	18425.96 mt

Source: Department of Agriculture, Wenchi Municipality.

3.2 The Economic Contribution of Cashew to the Livelihood of Farmers

The study revealed that the topmost source of income to the greater proportion of the respondents in the study area was cashew (56.75%). Formerly, maize [14] was the major occupation that provided economic reward to the farmers in the Municipality. Maize currently ranked second (25.50%) followed by yam (11.5%) according to the respondents. On gender bases, 58.8% of female cashew farmers placed cashew first whereas maize was graded second (21.6%) which was not all that different from their male counterparts about cashew (56.4%) and maize (26.1%). This agrees with another study by [1] in Guinea Bissau that cashew is the most important source of monetary income, in addition to being the core of both economic performance and poverty reduction. Other beneficiaries of cashew production were mostly women who handpicked the nuts and the local buyers. On average, female labourers could take away GHS 20 (US$3.47) a day for their labour. The local buyers were also in two categories; those who used their own capital and those who received funding from oversea expatriates to purchase the nuts. Cashew was source of livelihood to these "middlemen" (informants). However, only nuts of the fruit were sold (100%), while the apple was thrown away (0%).

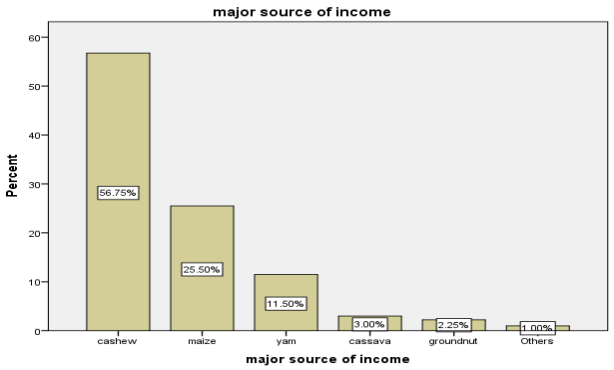

Figure 2. the major source of income to respondents

The study also revealed that majority of the respondents enjoyed much income from cashew in a given farming season. A greater proportion of respondents received a substantial amount of money between GHS 3,000.00 and GHS 4,000.00 (US$520- 693) (24%) within a farming season while others could accrue over GHS 5,000.00 (US$ 869) (23.3%). According to key informants, a cashew farmer could harvest an amount of GHS 7,350.00 per hectare (i.e. GHS 3,000 per acre) in a farming season if sales were favourable and the trees were mature (above 7 yrs.). It was also recognised that there was a discrepancy concerning the money both genders received. Among male cashew farmers who obtained GHS 5,000.00 during a farming season, was higher (27.5%) than their female counterparts (3.9%). Concerning GHS 3,000-4,000 threshold, among the male farmers, 22.9% were captured as against 23.5% of females. Also, at the lower range (GHS 100-900), the study showed 20.9% of male cashew farmers as against 39.2% female farmers. This revealed that the chunk of the female farmers did not receive much money as compared to the male farmers. The study again showed that the average cashew farmland for female farmers was 1 ha (3 acres) whereas that of the males was 2 ha

 DOI: https://doi.org/10.30564/jasr.v3i2.2010

(5 acres). There was a statistically significant relationship between gender and farm size $p< 0.05$ (0.003) and income received by cashew farmers and farm size $p< 0.05$ (0.000). Hence, male farmers were found to have better economic muscles than female cashew farmers when it came to cashew benefits.

3.3 The Shift of Farmland Use from Food Crop to Cashew Production and Its Implication for Food Security

3.3.1 Factors

The major factor endangering food security in the study areas was found to be the conversion of lands meant for food crop to cash crop (cashew) cultivation. About 71% of the respondents opined that they had expanded their cashew lands, another 41.0% had turned their food crops' lands to cashew farms, and 10.5% of the cashew farmers purchased their farmland from food crop farmers. The study found a correlation between the expanded farmland for, and output in cashew production and a corresponding declined in farmlands for, and output in maize [the dominant food crop] production in the Municipality. In other words, as farmland for cashew production and output in cashew production increases, food insecurity in the municipality also increases.

The study established the factor for the adverse impact of the increasing cashew production on food insecurity in the area. In-depth information elicited from farmers revealed that emerged the adverse correlation between the increasing cashew production and dwindling food security in the study area has to do with the fact that cashew production has compromised the traditional intercropping farming practice in the areas which allow framers to grow a variety of food crops on the same land to ensure the availability of a variety of food for rural households' upkeep throughout the year. The use of intercropping has been a major innovative indigenous farming practice that has helped the rural agricultural dependent folks to navigate extreme poverty, especially, the lack of money by saving their monies that would have gone into buying certain foods items. Through intercropping, farmers were able to cultivate and store a variety of food items, especially maize and beans and gari (processed cassava) for families used throughout the year. However, due to the shift to cashew production, active intercropping has become impossible when the cashew trees are about three to four years. The thick canopied cashew farms deny farmers the opportunity to continually intercrop cashew trees with food crop like cassava, maize, yam, groundnut with the cashew trees. The diminishing opportunity for intercropping was found to be contributing to food insecurity and exacerbating poverty in the study Municipality, especially among women, who are mostly the food crop farmers as the food crop farmlands are taken over by cashew trees, grown mostly by the men. This is because cashew dominated farmers are spending more money to buy food items, including locally produced ones which they could otherwise have produced, thereby dwindling any income they might have made from cashew. It, therefore, emerged that before the graze for cash production in the areas, although the rural farmers where poor in terms of purchasing power and access to social amenities, they were not poor when it comes to their resourcefulness in producing food locally to feed their families. However, the study found that climate change adaptability concern was found to have introduced a new set of risks including crop failure due to changing rainfall pattern and increasing incidence of pest invasions forcing the rural folks to shift from maize to cashew production.

The study found that farmers motivation for shifting from food crop to cashew production in the study area is not precipitated on a high income or stable market prices for cashews per se, but more of climate change adaptability concerns. According to participants, prices of cashew nuts have been unstable, oscillating between GHS 7.00 (US$1.20) per kilo and GHS 2 (US$ 0.35) for the past four years. One farmer expressed his disappointment that; "*The buyers could start purchasing the nuts at GHS 7.00 but within a twinkling of an eye, the price would fall as low as GHS2.00*". In probing the motivation for the shift from maize to cashew production, the study found that the shift is occasioned by climate change adaptability concerns rather than better market prices for the cashew nuts. According to the farmers, the cashew crop is resilient than maize (the main food crop in the area) in adapting to the changing climate in the area. Additionally, the cashew crop is less prone to pest invasions compared to maize in the area. Besides, historical data on pests' invasion, particularly on maize, and a corresponding increase in pesticides use among farmers in the study Municipality, suggesting an increasing cost of production to the farmers and declining output. Linked to the issue of the effect of climate change on farmland use decision and food security is the changing rainfall pattern. The changing rainfall pattern is adversely impacting the rainfed smallholding farming in the area. [19] observed that food crops in Ghana are increasingly becoming vulnerable to erratic rainfall than cashew. The most susceptible crops to the changing climate according to the study were maize (52.3%), yam (15.0%), groundnut (13.5%), vegetables (10.0%) and cashew (2.3%).

DOI: https://doi.org/10.30564/jasr.v3i2.2010

3.3.2 Effects

The study found that food security among the rural folks had been seriously compromised due to the conversion of farmland from food crop to cashew farming. The study revealed that about 49.0% of the cashew farmers experienced a shortage of food supply in the lean farming season. Such farmers relied on food on the market (mostly imported from other areas). The high prices of such food item relative to cashew farmers' income level erode any gains in income they might have accumulated from the shift from food crop to cashew production. In the long run, the cashew farmers become even worse off than food crop farmers [as food crop farmers usually store most of their farm produced for a family used so that they can overcome escalated price during the lean season]. The growing incident of food poverty of the cashew farmers articulated aptly by one farmer as;

"The majority of us too buy even locally produce food during the lean season because we don't have enough maize and beans to store and cassava and plantain farmers to rely on in the dry season."

According to participants, lives of some of the cashew farmers become miserable as they resorted to demanding *"soft loans"* from the buyers so that they could repay it with their nuts when the season got started. The high interest charged on such loans further worsens farmers' plight.

Additionally, the study found that female farmers have higher consciousness to food security and thus less propensity to shift from food crop to cashew crop production compared to men. The less motivation for the female farmers to shift from food crop to cashew crop does not suggest a low appetite for taking risks, instead, it is because females were found to have higher consciousness to family food security. The higher female consciousness to food security was found to have a link to the traditional role of the Ghanaian women in the extended family setting. In Ghanaian traditional setting, women are not just a caregiver, but they have a responsibility to feed the family with or without the support of the men or household heads. Hence, in the Akan ethnic group in Ghana, the title for women is *Maame* (mother) which translate as *my stomach is full*. This is further supported by our general field observation that the male farmers tend to have more apatite from cash crop production including cashew, cocoa and oil palm because its income comes in bulk in a given season of the year compare to food crop whose income comes in bits and pieces, throughout the year. However, cash crop farmers became venerable and poor in the off-season of those annual crops. Although the study found that female farmers have higher consciousness to food security and thus less propensity to shift from food crop to cashew crop production compared to men, they are the most severely hit group regarding the increasing shift of land use from food crop to cashew production. This is because women have little say on land use decision making at home and have less ownership of the farmlands compared to the men.

In total the general impact of the Shift of farmland from food crop to cashew production on food security as summarised in Figure 3 indicates that about 49% of respondents [farmers] are experiencing food insecurity.

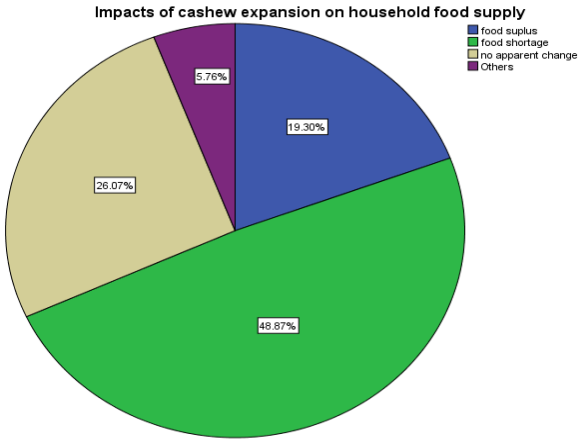

Figure 3. Impacts of expansion of cashew lands

Additionally, Table 2 also summarises the general problems confronting small-holding farming food and cash crop farming in the study area.

Table 2. Problem of cashew farming

Item	Frequency	Per cent	Cumulative Percent
unavailability of land	65	16.3	16.3
Unstable price	136	34.0	50.3
High temperature	8	2.0	52.3
Lack of capital	101	25.3	77.5
rainfall	43	10.8	88.3
Thieves	38	9.5	97.8
labourers	9	2.3	100.0
Total	400	100.0	

The study also found that the growing rural food insecurity caused by climate change adaptability concern of a shift from food crop to cash crop production in the study Municipality is contributing to the surge in rural-urban and north-south migration pattern in Ghana. This finding affirms [17] that increasing rural-urban migration in Ghana is linked to dwindling rural agricultural productivity, which the authors also linked it to the effect of climate

 DOI: https://doi.org/10.30564/jasr.v3i2.2010

change. The high rural-urban migration in Ghana the authors argued has, in turn, created a development challenge called "double jeopardy of rurality" in Ghana. A situation where rural areas are experiencing slow socio-economic development due to loss of human capital to urban Ghana and are also indirectly paying for the cost of overcrowding in the cities caused by the rural-urban migration, evidenced by skewed resources allocation in favour of urban areas to combat urban sanitation and housing deficit.

4. Conclusion

The study sought to analyse the impact of cashew farming on food security of the people of Wenchi Municipality. The findings of the study attest to and reflect the unequal benefits and challenges posed by the cashew farming between individuals and genders. The data from the Municipal Assembly confirms the exponential increase in production and expansion of cashew lands and dwindling food crop output. Even though cashew farmers accrued more income than food crops farmers at a go, food crop farmers were found to have better food security throughout the year and are comparatively better off than the cashew farmers whose income get eroded by increasing food prices in the lean season. Although the study found that female farmers have higher consciousness to food security and thus less motivated to shift from food crop to cash (cashew) crop production compared to men, the females are the most severely hit group bearing the brunt of the shift of land use from food crop to cashew production because they carry more responsibility of feeding the family, hence have little say on land use decision making at home and have less ownership and thus access to farmlands compared to the men. The study concludes that climate change adaptability concern was found to have introduced a new set of risks including food crop failure due to changing rainfall pattern and increasing incidence of pest invasions forcing the rural folks to shift from maize to cashew production. Further investigation on how to mitigate the impact of climate change on rural food security is very crucial especially regarding improved food crop seeds tailored to the specific climatic context and innovative farming practices that will help small-holding farmers to navigate climate change effect on food crop production to ensure rural food security and sustainability. This crucial as rural food insecurity caused by climate change is causing a surge in rural-urban and north-south migration in Ghana and, global South and North migration.

Competing Interest

Authors have declared that no competing interests exist.

Acknowledgement

The authors would like to show their profound gratitude to the people of Wenchi Municipality for their immense participation in this paper for sharing their pearls of wisdom with us during the course of this research work. The support of the Department of Agriculture of the Municipality is also much treasured.

We would also like to express our in-depth appreciation to our field workers most especially Mr. Seth Addae and his entourage such as Mavis Gaazienye, Solomon Bayor, Hibert Doglier, David Korgbiele and Michael Diibu. We say kudos to your immense support beyond measure.

Other personalities which we cannot forget are Dr Rosina Kyerematen, Dr Robert Ahenkan (all of University of Ghana) Hagar Danquah, Crosby Adjei, Benita Adjei and Mad. Georgina Kodom.

References

[1] Monteiro F. Catarino L., Batista D. Indjai B., Duarte M. C. and Romeiras M. M.. Cashew as a High Agricultural Commodity in West Africa: Insights towards Sustainable Production in Guinea-Bissau, 2017. www.mdpi.com/journal/sustainability (accessed 22nd January 2020)

[2] Ghana Statistical Service, National Analytical Report 2010 Population and Housing Census Ghana Statistical Service, 2012.

[3] Ghana Statistical Service (2015) Composite Budget of the Wenchi Municipal Assembly for 2015 Ghana Statistical Service, 2016.

[4] African Cashew Initiative. A Value Chain Analysis of the Cashew Sector in Ghana; Deutsche Gesellschaft für Technische Zusammenarbeit GmbH (GTZ) International Foundations, 2010.

[5] FAO. Gender inequalities in rural employment in Ghana. An overview. Food and Agricultural Organization, 2012. Retrieved from: http://www.fao.org/docrep/016/ap090e/ap090e00.pdf (assessed on 18.12.08)

[6] Ghana Living Standard Survey- GLSS8, 2018. http://www.statsghana.gov.gh/nada/index.php (assessed on 30th March, 2020)

[7] World Bank. The World Bank Annual Report 2013. Washington, DC. © World Bank, 2013. https://openknowledge.worldbank.org/handle/10986/16091 License: CC BY 3.0 IGO.

[8] Salam, M.A. Peter, K.V. Cashew-A Monograph; Studium Press (India) Pvt. Ltd.: New Delhi, India, 2010.

[9] Rabany, C., Rullier, N., Ricau, P.. The African Cashew Sector in 2015, 2015. Available online:

  DOI: https://doi.org/10.30564/jasr.v3i2.2010

http://www.rongead.org/IMG/pdf/african_cashew_market_review_rongead_ica_2015 (accessed on 14th March 2020).

[10] Dedzoe C.D., Senayah J.K., Assiamah R.D. Suitable agro-ecologies for cashew (Anacardium Occidentale L.) production in Ghana. West Afr J Appl Eco., 2001, l 2: 103-115.

[11] Wongnaa C. A.1, Awunyo-Vitor.D. Profitability analysis of cashew production in Wenchi municipality in Ghana, 2013.

[12] Ghana Statistical Service (GSS). Statistics for Development and Progress: Gros Domestic Product 2014, 2016. Retrieved on 12th January 2016 from: www.statsghana.gov.gh

[13] Anlimachie, M.A, Avoada, C.Socio-Economic Impact of Closing the Rural-Urban Gap in Pre-tertiary Education in Ghana, (in-print), International Journal of Educational Development, 2020.

[14] Adjei-Nsiah S., Kermah M.. Climate Change and Shift in Cropping System: From Cocoa to Maize Based Cropping System in Wenchi Area of Ghana. British Journal of Environment & Climate Change, 2012, 2(2): 137-152, Sciencedomain international. www.sciencedomain.org

[15] Adjei V., Kyerematen R.. Impacts of Changing Climate on Maize Production in the Transitional Zone of Ghana. American Journal of Climate Change, 2018, 7: 463-476. https://doi.org/10.4236/ajcc.2018.73028

[16] Khan, H., Ali, F.. Measurement of Productive Efficiency of Tomato Growers in Peshawar, Pakistan. Agric. Econ. CZECH, 2013, 59(8): 381-388. ISSN: 0139-570 X.

[17] Amoako-Mensah, T., Anlimachie, A. M., Adu, B. S., Elorm, E. A.. Out-migration and the Double Jeopardy of rurality in Ghana. An integrated approach to rural development. European journal of geography, 2019, 10: 50-67.

[18] Osei-Akoto, S., Topper, C.P., Swatson, E.. Status of cashew production in Ghana and agronomic options for increasing production by smallholder farmers. Paper presented at Ghana Institute of Horticulture Annual Conference, 2005.

[19] Adjei V., Kwantwi L. B.. Maize and Cashew Farming in the Face of Climate Change Variability in the Transitional Zone of Ghana: A Case Study of Nkoranza South Municipality American Journal of Environmental Sciences, 2019.

 DOI: https://doi.org/10.30564/jasr.v3i2.2010

BILINGUAL PUBLISHING CO.
Pioneer of Global Academics Since 1984

Journal of Atmospheric Science Research
https://ojs.bilpublishing.com/index.php/jasr

ARTICLE

Global Warming and Its Multiple Causes

Romdhane Ben Slama*

Higher Institute of Applied Sciences and Technology of Gabes (ISSAT), University of Gabes, Tunisia

ARTICLE INFO

Article history
Received: 17 June 2020
Accepted: 16 July 2020
Published Online: 30 July 2020

Keywords:
Greenhouse effect gases
Global warming
Infrared emission
Heat of combustion

ABSTRACT

The global warming which preoccupies humanity, is still considered to be linked to a single cause which is the emission of greenhouse gases, CO_2 in particular. In this article, we try to show that, on the one hand, the greenhouse effect (the radiative imprisonment to use the scientific term) took place in conjunction with the infrared radiation emitted by the earth. The surplus of CO_2 due to the combustion of fossil fuels, but also the surplus of infrared emissions from artificialized soils contribute together or each separately, to the imbalance of the natural greenhouse effect and the trend of global warming. In addition, another actor acting directly and instantaneously on the warming of the ambient air is the heat released by fossil fuels estimated at 17415.1010 kWh / year inducing a rise in temperature of 0.122°C, or 12.2°C / century.

1. Introduction

Global warming, an object of current world occupation is attached above all to the greenhouse effect (anthropogenic), due to human activity, and this by the combustion of fossil energies (coal, oil and gas) and their emissions of greenhouse effect gas. This warming should prompt us to look for the cause to avoid it or provide remedies.

2. Greenhouse Effect and CO_2 Emission

In fact, the annual global consumption of energy amounts to around 15,000 Mtoe generating the emission of almost 35,000 MtCO2e (Figure1 à 3) [1]. This quantity is added to atmospheric gas (air and humidity) to create a surplus of anthropogenic GHGs causing global warming, the COP 21 ... 26 of which strives to reduce its effects by encouraging states to limit their CO_2 emissions. Although the share of CO_2 emitted represents only 0.0007% of the atmospheric mass, but it reaches 2.3% of the mass of CO_2 contained in the atmosphere.

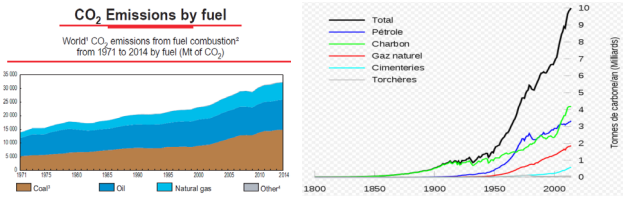

Figure 1. Global CO_2 emission [1]

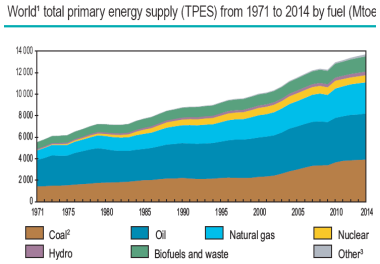

Figure 2. Evolution of energy consumption world [1]

**Corresponding Author:*
Romdhane Ben Slama,
Higher Institute of Applied Sciences and Technology of Gabes (ISSAT), University of Gabes, Tunisia;
Email: Romdhaneb.slama@gmail.com

DOI: https://doi.org/10.30564/jasr.v3i2.2013

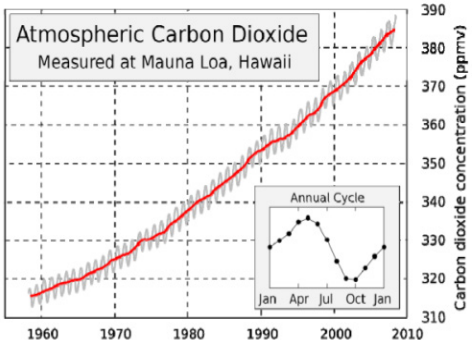

Figure 3. Evolution of concentration of particles in the air

However, other considerations must be taken into account to create the greenhouse effect, although the name is not perfect, because an agricultural greenhouse does not heat only by the plastic or the glass that envelops it because if we opens it, it cools, so it's the absence of transfer by convection with the outside by the immobilization of the air in its movement and not the radiation that heats a greenhouse [2-6]. For the earth, on the contrary: it is the radiative imprisonment of this planet which heats it. Capturing the air of the earth makes no sense.

GHGs are selective: they allows short wavelength sunlight [0.25 to 2.5m] to pass through the earth and are opaque to terrestrial infrared emission [5 to 50m] (Figure 4) towards space. Thank goodness this is necessary for life on earth by maintaining an average temperature of 15 ° C currently, against -18°C in fact the absence of the greenhouse effect.

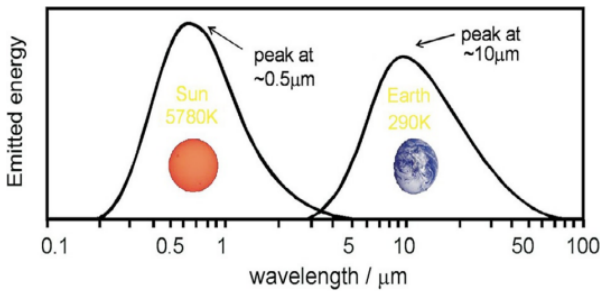

Figure 4. Solar and terrestrial radiative spectrum

However, "human activity" has favored CO2 emissions, causing a climatic imbalance, minimal as it is, but sufficient to cause the melting of the polar ice, the rise in sea level, the retreat of the coastline in many areas. coastal regions, the advancing desert, and climate change in general. Some believe that we must adapt to these climate changes. Conversely, we think it would be more rational for the future of the earth to stop the cause of this scourge in the first place, like the various conferences of the parties of the United Nations COP by limiting CO2 emissions.

3. Greenhouse Effect and Infrared Emission from Earth and Artificial Soils [7]

So far, much has been written about the greenhouse effect linked to GHG emissions. If now we make the analogy with the greenhouse effect used in a solar thermal collector (Figure 5), we observe that the glazing which creates the greenhouse effect opposes IR radiation all the more powerful as the absorbing surface is dark color (black in this case).

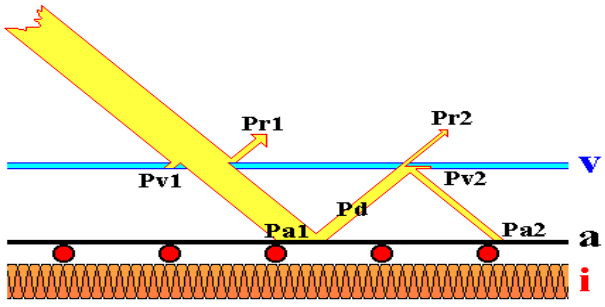

Figure 5. Analogy with the greenhouse effect of a solar thermal collector

So for the earth, all artificial soils (roads, roads, buildings), dark in color will absorb sunlight and re-emit in far IR which does not cross the atmosphere, all the more if this is polluted.

Figure 6. Examples of dark colored roads and buildings participating in the IR emissions to which the GHGs are opaque

Another action which therefore remains to be carried out and to develop the above studies concerns the infrared radiation emission from artificial soils. Here again, if this emission is natural, it can only be beneficial for humanity (maintains an average temperature on earth at +15°C instead of -18°C without natural greenhouse effect). However, by the artificialisation of soils, (paved roads, roads, dark colored buildings, etc.), (Figure 6), terrestrial infrared emissions are closely related to the increase in

 DOI: https://doi.org/10.30564/jasr.v3i2.2013

the absorption coefficient of solar radiation by the artificial soils and the decrease of the albedo coefficient. This infrared emission parameter not "yet" currently taken into account by the COP has, in our opinion, a responsibility, at least comparable to that of CO2 emissions, to say the least, because if the IR emissions of the earth increase, but with an atmosphere "healthy" there would be radiative imprisonment and therefore global warming. The efforts to be deployed must therefore be commensurate with the climatic issue in question. Indeed, a soil is naturally light in color, and s 'It is covered with plants, which absorb less than 1% of the incident solar radiation. Conversely, a black tarmac road absorbs a large amount of solar energy (90%), heats up and reemits in the far infrared which is absorbed by the atmosphere and partially returned to the earth causing the radiative imprisonment popularly called: greenhouse effect.

4. Greenhouse Effect Generated by the Combustion of Fossil Fuels

Apart from GHGs and their interaction with terrestrial (natural and artificial) infrared emissions leading to global warming, another factor of global warming is not addressed in the analyzes of global warming, despite its evidence and its direct impact on the heating of surrounding air, this time it is not the effect of CO2 which is a product of combustion, but rather the direct effect of combustion (heat given off by the flame) on the heating of the air in direct contact and therefore the increase in atmospheric temperature.

Knowing that approximately 15,000 Mtoe are burned annually, representing a calorific energy calculated by the product of the calorific power by the mass of the fuel, that is: PCI.m.

The oil PCI is 10 kWh / liter with a mass volume of 1161 liter / toe; thus PCI.m = 15.10^9 x 1161 x 10 = 17415 10^{10} kWh / year.

This energy risks heating the atmospheric air according to the energy balance:

(PCI.m) petroleum = (m.Cp.DT) air

With mair = $5.14.10^{18}$ kg and Cp air = 1000 J / (Kg. ° C)

This generates an annual temperature rise of 0.122 ° C.

So after ten years (quickly gone!) Global warming would have exceeded 1 ° C, which is not nothing, compared to the objective set by the COP 21… .26 to limit global warming at 2 ° C per century.

So terrestrial global warming is at fortiori, indirectly caused by the greenhouse effect (due to both GHG emissions and infrared radiation from artificialized soils), combined with direct heating of the air following the heat released by burning fossil fuels.

This is what has been observed in recent years, and already at the start of 2020, the temperatures measured for example in France exceed 2.5 ° C the averages of past decades.

And global warming is almost a vicious circle, because the melting ice of the north and south poles will promote the absorption of solar radiation by reducing albedo and amplifying the natural terrestrial infrared radiation emissions. On the other hand, there would be an increase in GHGs generated by the microorganisms that will take place due to the change in vegetation.

Even renewable energies, used on a very large scale such as the thermal conversion of solar energy can contribute to heat the climate directly and indirectly by the emission of infrared radiation.

The best energy is the one we don't use.

5. Conclusion

To meet the objective of 2°C of global warming per century, it is necessary:

(1) Take an interest not only in limiting CO2 emissions worldwide (use of renewable energies), but also in: Limit the commercialization of soils, especially towards dark-colored buildings

(2) Limit the artificialisétion of soils, especially towards dark-colored buildings which absorb solar radiation and emit into the IR, such as roads, buildings, etc.

(3) Reduce the combustion of fossil fuels that heat atmospheric air and improve the efficiency of energy systems.

References

[1] www.iea.org

[2] Ben Slama, R. Green House Effect vs. Infrared Radiation Emissions. Journal of Climatology & Weather Forecasting, 2016, 4: 1. http://dx.doi.org/10.4172/2332-2594.1000161

[3] Ben Slama, R. L'Effet de serre et les radiations infrarouges des zones urbaines et goudronnées sombres. International Congress on Energetic and Environmental Systems (IEES-2017). Djerba, Tunisia, 2017, 17-19.

[4] Ben Slama, R. Role of the dark surfaces of cities on the greenhouse effect increase. Int. Conf. on Sustainible development, Ottawa, Ontario Canada, Visioconference, 2017.

[5] Ben Slama, R. Effet de serre vs émissions terrestres de rayonnement infrarouge : l'effet de serre n'est pas du qu'au dégagement des Gaz à Effet de Serre. Colloque 604. Congres de l'ACFAS 85éme édition, sur le

DOI: https://doi.org/10.30564/jasr.v3i2.2013

thème : Regards croisés sur l'adaptation aux changements climatiques dans le transport terrestre : Quelles formes, insuffisances et nouvelles pistes ? Mercredi 10 Mai 2017 ; Université McGill, Montréal, Québec, Canada, 2017.

[6] Ben Slama, R. Impact of the Artificial Surfaces Sunk on the Global Warming by the Absorption of the Solar Radiation and the Albedo Coefficient Modification. Journal of Climatology and Weather Forecasting, 2018, 6: 2.
DOI: 10.4172/2332-2594.1000230

[7] Ben Slama, R. Modification of the terrestrial albedo following the absorption of the solar radiation by the dark artificial surfaces and its influence on the green house effect. Physics & Astronomy International Journal. 2018, 2(6).

 DOI: https://doi.org/10.30564/jasr.v3i2.2013

BILINGUAL PUBLISHING CO.
Pioneer of Global Academics Since 1984

Journal of Atmospheric Science Research
https://ojs.bilpublishing.com/index.php/jasr

ARTICLE

Characterization of $PM_{2.5}$ Mass Concentration in the Onshore of Sanya, China

Ping Wang[1,2*] Chao Han[1] Youzhi Zhao[1] Wenci Ding[1] Zengzeng Li[1]

1. School of Science and Technology, Hainan Tropical Ocean University, Sanya 572022, China
2. Key Laboratory of Aerosol Chemistry & Physics, Institute of Earth Environment, Chinese Academy of Sciences, Xi'an 710061, China

ARTICLE INFO

Article history
Received: 13 July 2020
Accepted: 20 July 2020
Published Online: 30 July 2020

Keywords:
Sanya
$PM_{2.5}$
Carbonaceous aerosol
Biomass burning

ABSTRACT

Numbers of real-time data (E-BAM) of $PM_{2.5}$ were collected in the period from Jan 8th 2012 to Jan 1st 2013 at the laboratory of Tropical Ocean University (Sanya, China). The average mass concentration was 19.7 μg/m³. The highest 40.5 μg/m³ in October compared to the lowest 14.1 μg/m³ in July. From a seasonal perspective, the average $PM_{2.5}$ mass concentration in fall and winter are relatively higher than that in both spring and summer. On the basis of satellite map of fire points and backward trajectories of the air masses, we primarily deduced that the $PM_{2.5}$ in Sanya may be caused by the biomass burning and industrial pollutants from the area of Pearl River Delta of China and the Indo-China peninsula (e.g. Vietnam, Laos).

1. Introduction

Fine particulate matter ($PM_{2.5}$) has been identified as the main cause of smog, posing a series of problems to China, not only aroused public health concern, but also led to other issues. High concentration of $PM_{2.5}$ could lead to the reduction of visibility, which can be hazardous to driving and shipping [1,8].

The increase in $PM_{2.5}$ has already become a severe problem in China and even the whole world. The research status of $PM_{2.5}$ in China is as follows, the physicochemical characteristic of $PM_{2.5}$ has been already studied years before [10], and the formation mechanism of $PM_{2.5}$ was also researched [14]. Furthermore, in 2014, Chinese Academy

**Corresponding Author:*
Ping Wang,
School of Science and Technology, Hainan Tropical Ocean University, Sanya 572022, China;
Key Laboratory of Aerosol Chemistry & Physics, Institute of Earth Environment, Chinese Academy of Sciences, Xi'an 710061, China;
Email: wangpingalong@163.com

DOI: https://doi.org/10.30564/jasr.v3i2.2134

of Sciences found for the first time that the great contributions of high secondary aerosol to particulate pollution during haze events in China [4]. Biomass combustion is one of the main sources of fine particulate ($PM_{2.5}$) in Sanya. Mostly the $PM_{2.5}$ was emitted from open fire places, pallet stoves and boilers, wood, and crop waste [7]. Low combustion efficiency could cause high organic emissions and arouse the discharge of toxic substances.

Sanya is a coastal city located in southernmost China, enjoys a high level of reputation for its air quality compared with the other cities in mainland of China. The World Health Organization air quality guidelines state that the annual mean concentration of $PM_{2.5}$ should be below 10μg/m^3 [12] whereas the mass concentration of $PM_{2.5}$ in Sanya was around 19.73μg/m³. Sanya is the only islet of China, where the air quality was easily affected by the monsoon climate. In addition, the air quality in Sanya is prone to be impacted by the biomass burning of the Indo-China peninsula and the industrial pollutants from the area of Pearl River Delta in China due to the air mass transportation [2]. Furthermore, as a typical transitional zone between land and ocean, it is worth conducting a series of research. So far, only limited of $PM_{2.5}$ research have been done throughout the world. In Sanya, both motor vehicle and biomass burning are the main emission source of $PM_{2.5}$, contributed PAH (polycyclic aromatic hydrocarbon) up to 60% of total emission [11]. A biomass burning research has been conducted in Jianfengling of Hainan Island, which indicates that the emission of toxic substances in winter is much higher than that in summer [15]. The study of characteristics of carbonaceous aerosol in Sanya has never been conducted in the previous researches.

The objectives of this study are to review available $PM_{2.5}$ and meteorological data and apply some proper techniques such as quantitative analysis and backward trajectories analysis in order to characterize the mass concentration of $PM_{2.5}$ in Sanya. Here, apart from analyzing the correlation between $PM_{2.5}$ mass concentration and meteorological factors, we also use backward trajectories and satellites images of fire points to trace the source of $PM_{2.5}$ caused by biomass combustion.

2. Methodologies

2.1 Sampling Site

The measurements of $PM_{2.5}$ were taken at the Department of Tropical Eco-environment Protection (Hainan Tropical Ocean University, 18°18'N, 109°31'E), situated in the northeast of the city of Sanya. Figure 1 illustrates the geographical location of Sanya. Sanya has a tropical coastal monsoon climate with a very humid and hot summer. Its ambient yearly humidity (AH) is generally around 90% in summer, and even higher (up to 95%) during the monsoon season (July-October). the AH is generally higher, around 95% of a month. Sanya receives a huge amount of rainfall every year with an average annual rainfall of 1263 mm and 90.2% of it concentrates in the monsoon season (June-October), namely rainy season (Weather Service of Sanya). As in the mainland of China, season was defined according to the meteorological division of seasons of 3 months each (spring: March–May, summer: June–August, fall: September–November, winter: December–February). We use an E-BAM (Environmental Beta Attenuation Monitor) particulate monitor to measure $PM_{2.5}$ mass concentrations, ambient temperature and relative humidity of the whole year of 2012, data have also been collected throughout the year. The meteorological patterns are quite different, the maximum temperature occurred in summer, at an average of 29 degrees Celsius. Similarly, the relative humidity (RH) also saw a high in summer, accounted for 95% in average, ranging from 87% to 99%. Compared to the winter, only around 23 degrees Celsius of temperature and 85% of RH.

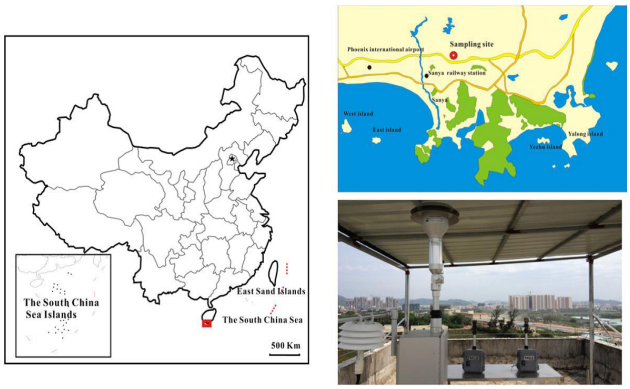

Figure 1. Location of the sampling site in Sanya, China

2.2 Methods

In total, 8132 pieces of data ($PM_{2.5}$ measurements) were collected from 2012.01.08 to 2013.01.01 on the top of the building for the Department of Science Studies, Hainan Tropical Ocean University. Data were not available during the monitor calibration and severe weather conditions, such as typhoon, the data will be analyzed on a scale of month, the individual missing data would be ignored. 24-hour averaged temperature, relative humidity (RH), wind speed (WS), and precipitation data from 2012.01.01 to 2012.12.31 were obtained from the Meteorological Bureau of Hainan province.

DOI: https://doi.org/10.30564/jasr.v3i2.2134

2.2.1 E-BAM

The E-BAM samples the air and reports the measurements of samples continuously every minute. With the application of Beta Attenuation, E-BAM eliminates the outdated method of manual filter collection and weighing, and thereby facilitates the measurements of particulate matter. $PM_{2.5}$ concentration data were collected on hourly frequency, ambient temperature and relative humidity data were simultaneously collected. The E-BAM has been programmed to measure at virtually all times. Current data, historical data, and status information are available at all times without interrupting normal E-BAM operation.

2.2.2 Back Trajectories and the HYSPLIT4 Software

HYSPLIT4 model analysis was conducted to focus on the trajectories of airmass. Backward trajectories of the air mass are closely correlated to the wind direction and pollutants transmission path, which is helpful for us to analyze the spatial distribution of PM2.5. Forward trajectories were calculated by HYSPLIT4 (Hybrid Single-Particle Lagrangian-Integrated Trajectory) modeling software. This software was freely accessed through the Air Resource Laboratory (ARL) of the National Oceanic and Atmospheric Administration (NOAA). The HYSPLIT4 model referenced archived meteorological data for computing backward trajectories.

The vertical distribution of $PM_{2.5}$ ranging from 8m-300m in the atmosphere [9], due to the fact that airmass movement in the low altitude could be affected by buildings and anthropogenic activities, we will choose 100m as our primary height settings for conducting calculation of backward trajectory. In order to have a stable pattern of wind direction to trace the $PM_{2.5}$ sources of Sanya, we will also illustrate the airmass movements around 500m. The result could illustrate the airmass moving trajectory in the set period of time at 100m, 500m.

2.2.3 Active Fire Map

Humans use fire as a tool in slash-and-burn agriculture to speed up the process of breaking down of unwanted vegetation into the soil. Small forest fires also occurred in winter (November to March) in Southern China, including Yunnan, Guangdong and Guangxi Autonomous Regions [6]. In this case, the $PM_{2.5}$ may increase by these activities. It has the possibility that the local $PM_{2.5}$ could to some extent, transported by wind to other provinces like Hainan province, so we decide to combine the local $PM_{2.5}$ data and fire map to see whether there is a correlation between airmass trajectory and fire map.

The Figures of Active Fire and thermal anomalies were captured and compiled by TERRA/MODIS (NASA data pool). MODIS fire location data are distributed in a variety of forms (e.g. interactive web mapper, GIS, Google Earth, text files) through the Fire Information for Resource Management System (FIRMS) at the University of Maryland. Besides, the VIIRS (Visible Infrared Imaging Radiometer Suite) satellite data were also collected. The current MODIS and VIIRS satellite data could be downloaded from https://firms.modaps.eosdis.nasa.gov/.

3. Results and Discussion

3.1 Daily, Monthly, Annual Variations of $PM_{2.5}$ Mass Concentrations

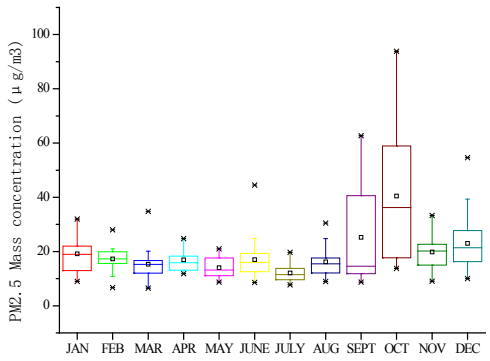

Figure 2. The Monthly variation of $PM_{2.5}$ mass concentration in 2012

The variation of average $PM_{2.5}$ mass concentration ranked as October (40.5μg/m³) > September (25.2μg/m³) > December (23μg/m³ > Rest of months). High values occurred during October and took up the most part of $PM_{2.5}$ mass concentration in Sanya in 2012, with a high of 93.8μg/m³. The Figure 2 of $PM_{2.5}$ mass concentration in October is remarkably higher than the rest of month, almost twice as much as that in September and three times as in rest of months. It is also noticeable that in the period from January to August, the contents of $PM_{2.5}$ are relatively lower than that in the period from September to December, which remained the same level from 14μg/m³ to 19.2μg/m³. Since the development of industry was never allowed by the policy of Chinese government. And this region is not like some northern cities which need coal burning for heating. We deduced that the $PM_{2.5}$ in October are from somewhere else. It is also noticeable that the maximum $PM_{2.5}$ value is not connected with the box in February, March, June, August and December, which may be caused by the data outlier in these months.

DOI: https://doi.org/10.30564/jasr.v3i2.2134

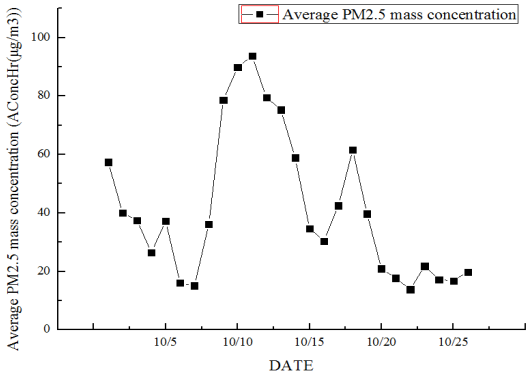

Figure 3. Daily $PM_{2.5}$ mass concentration in October, 2012 and Chinese/USEPA standard

Figure 3 provides the information of daily average $PM_{2.5}$ concentrations in October. The US Environmental Protection Agency (EPA) set a standard in 1997 which indicates the diurnal $PM_{2.5}$ ($\leq 35\mu g/m^3$), we can observe from the data in October that only 12 days (46%) have reached the EPA standard. In comparison with the standard (diurnal $PM_{2.5} \leq 75\mu g/m^3$) from Ministry of Environmental Protection of The People's Republic of China, only 5 days (19%) exceeded the standard. From the graph, the highest measurement occurred on 11st Oct, around $93\mu g/m^3$, compared to 7th Oct, only accounted for $15\mu g/m^3$. Overall, the $PM_{2.5}$ mass concentration in October fluctuated to a large extent reached the maximum at 11st Oct and then fell to the same level as 7th Oct at 26th Oct.

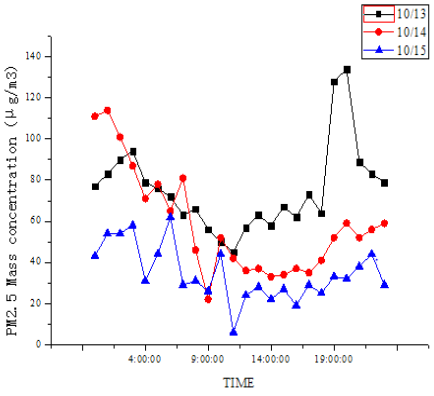

Figure 4. Hourly $PM_{2.5}$ variations on 13th, 14th, 15th Oct, 2012

To examine the diurnal variations in $PM_{2.5}$ mass concentration. We used Hourly $PM_{2.5}$ contents data (collected by E-BAM) to make a line chart above (Figure 4). Overall, $PM_{2.5}$ mass concentration in all three days were at a high level in the midnight, around $78\mu g/m^3$(10/13), $110\mu g/m^3$(10/14), $42\mu g/m^3$(10/15) respectively. Then the Figures saw a decrease from midnight to 5-8:00 a.m. After that, the contents of $PM_{2.5}$ have remained steady until 7:00 pm. In combination with the human activity, the increase of vehicles in the rush hour probably contributed some aerosol contamination including $PM_{2.5}$. Eventually, it saw an increasing trend from 7:00 pm to the following midnight.

3.2 Weather and $PM_{2.5}$

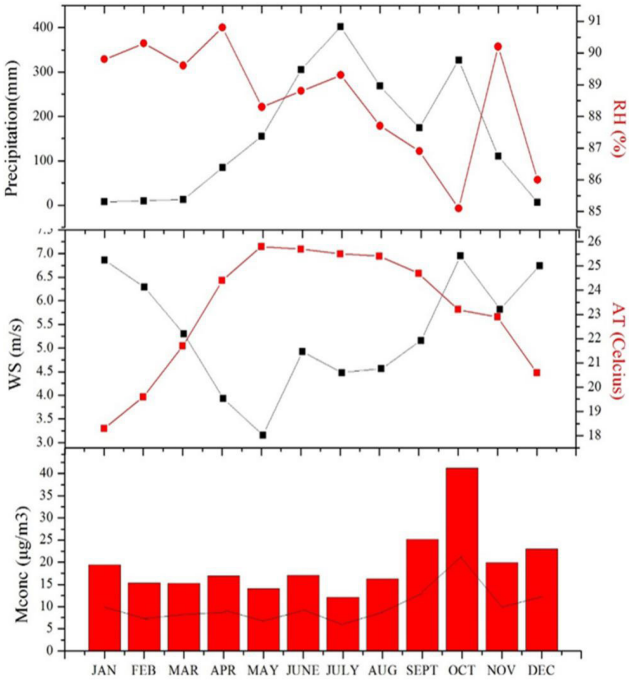

Figure 5. Monthly variation of major meteorological

Figure 5 illustrates Monthly variation of main meteorological parameters in 2012, including monthly average precipitation, relative humidity, daily wind speed and average temperature. The precipitation in winter (December, January and February) were the lowest throughout the whole year, around 7.4mm, 9.9mm, and 6.4mm respectively. It went higher from March (12.8mm) and saw the climax in July (402.2mm). Then the rainfall remained at the high level until November. In terms of relative humidity (RH), in every month, Sanya always maintained at a high level of that because Sanya is a tropical city and stand not far from the sea, the Figure 5 of RH were no less than 85% of a whole year. It has been observed that the wind speed in October were the fastest (6.95m/s), closely followed by January (6.86m/s) and December (6.74m/s), whereas the wind is usually calm from March to September, ranging from 3.16-5.82m/s. As regard daily mean temperature, the highest were in the range of April to September (24.4-25.7 ℃). Overall, the relative humidity, average temperature, and monthly precipitation were irrel-

DOI: https://doi.org/10.30564/jasr.v3i2.2134

evant to $PM_{2.5}$ mass concentrations. However, it is clearly from the charts that in the period from May to December in 2012, the variation of wind speed was more or less correlated with the $PM_{2.5}$ mass concentration.

3.3 Relationship between Active Fire and Backward Trajectories

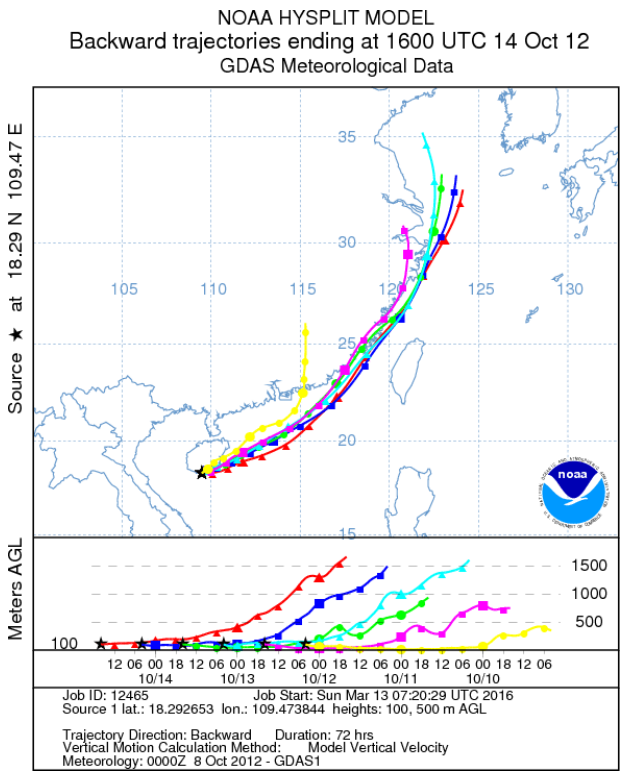

Figure 6. Backward trajectory of Sanya (18.29N 109.47E) in October, 2012

5-day Backward trajectories from the location (18.29N 109.47E) have been calculated using the HYSPLIT 4 model (HYbrid Single-Particle Lagrangian Integrated trajectory) (Figure 6). The certain trajectory that was created started at Tropical Ocean University (18.29N 109.47E) at (100,500) meters above ground level and was calculated back seventy-two hours.

The backward trajectory of 0000 UT from October 12, 2012 was chosen as an example for the path that air pollutant went because this trajectory began its journey in the Guangdong Province, where the industries well-developed and factories are scattered. Nevertheless, the rest of backward trajectories saw a same travel route that most of them were along with the coastal cities.

From the backward trajectory made above we can tell that airborne contaminant (100-500m) in Sanya in October 2012 were possibly transported from Guangdong Province and a series of coastal cities of China.

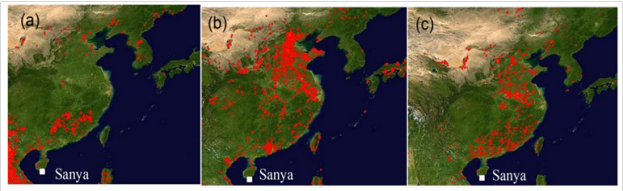

Figure 7. 8-day composite fire products during 22th February- 29th February 2012(a); 9th July-18th July 2012(b) and 7th October - 16th October 2012(c)

Figure 7 show the locations of actively burning fires around the world, detected by instruments aboard NASA satellites. The NASA MODIS global fire digital maps are calculated from Terra and Aqua MODIS data, designed primarily to serve the needs of the emissions modeling Community. The red dots illustrate fire and thermal anomalies detected by MODIS Aqua/Terra satellite. The yellow dots also present the fire and thermal anomalies in the set period of time; however, the data was collected from the VIIRS (Visible Infrared Imaging Radiometer Suite).

These fire products present a similar, locally coherent, spatio-temporal progression of burning. Each of these 3 fire maps accumulates the locations of the fires detected by MODIS on board the Terra and Aqua satellites and VIIRS over an 8-day period. Each colored dot indicates a location where MODIS detected at least one fire or thermal anomalies during the compositing period.

From the fire maps shown above, it is clear that during the period of 7th October - 16th October in 2012, the active fires occurred more frequently in those coastal cities of China than that in the February. However, the fire chances of coastal city in July was relatively lower than the chances in October.

In combination with the backward trajectory of the same period in October, there is a great chance that the airborne contamination including Particulate Matters were transported from the coastal cities of mainland of China.

3.4 Discussion

$PM_{2.5}$ particulate is scattered at different height, it could be transported by wind, and the transportation could be affected by aerosol optical properties, winds, relative humidity and also temperature [3]. Besides, other weather variation could have an impact on the transmission of atmospheric particles to some extent. For example, the precipitation amount could accelerate the sedimentation speed of particulate matter in the air [13]. The vertical distribution of $PM_{2.5}$ is from 8-300m, and the $PM_{2.5}$ amount at different height could be various [5,9]. The paper only simulated the backward trajectory at a height of 100m and 500m, the result may not be able to restore the transmis-

DOI: https://doi.org/10.30564/jasr.v3i2.2134

sion trajectory of all particulate matters in the air, anomalies caused by topography and constructions may exist in the airmass trajectory at lower height.

Other possible $PM_{2.5}$ sources exist in this city such as in winter, a substantial amount of people moving to Sanya city to spend the winter time because of less air pollution and higher temperature in this city. People from the mainland have brought a great mount of vehicles from other provinces for their commuting convenience, which could be a potential sources of aerosol pollutants. The sample were collected by the Hainan meteorological bureau in Hedong monitoring station which located near city center, in this case, the particulate data could be affected by the sudden increase of vehicles in Sanya city in winter.

4. Conclusion

The monthly and daily variations of the $PM_{2.5}$ mass concentrations were carried out using E-BAM aerosol contamination monitor the major findings of this present study are as follows:

(1) In the period of September-November in 2012, the $PM_{2.5}$ mass concentration increased remarkably compared to the rest of months, which hinted that whether there was a new source of pollution in Sanya or the $PM_{2.5}$ in fall were transported from somewhere else.

(2) The daily $PM_{2.5}$ mass concentration in October took up the most of $PM_{2.5}$ in 2012, only 46% days have reached the EPA standard ($\leq 35 \mu g/m^3$) but 81% met the Chinese $PM_{2.5}$ standard (diurnal $PM_{2.5} \leq 75 \mu g/m^3$).

(3) The correlation analysis between $PM_{2.5}$ concentration and meteorological factors indicated that the relative humidity, average temperature, and monthly precipitation were mostly irrelevant to $PM_{2.5}$ mass concentrations, but it saw some correlations between $PM_{2.5}$ contents and wind speed in the chart.

(4) Observed backward trajectory in combination with fire products in the same period of 2012, we primarily deduced that the aerosol pollution including $PM_{2.5}$ are come from Guangdong Province and the coastal cities of China.

Acknowledgments

This work was supported by Cooperation Project of Chinese Academy of Sciences and Sanya Government (2018YD14). It also partially supported by the National Natural Science Foundation of China (41867046), Hainan Provincial Natural Science Foundation of China (2019RC243), State Key Laboratory of Loess and Quaternary Geology (SKLLQG1830) and Key Laboratory of Aerosol Chemistry and Physics (KLACP2001), Institute of Earth Environment, CAS. We thank Giovanni online tools of the NASA Goddard Earth Sciences Data and Information Services Center (GES DISC).

References

[1] Cao, J.J., Zhu, C.S., Tie, X.X., Geng, F.H., Xu, H.M., Ho, S.S.H., Wang, G.H., Han, Y.M., Ho, K.F. Characteristics and sources of carbonaceous aerosols from Shanghai, China, Atmospheric Chemistry and Physics, 2013, 13(2): 803-817.

[2] Chang, T.J., Kao, H.M., Wu, Y.T., Huang, W.H. Transport mechanisms of coarse, fine, and very fine particulate matter in urban street canopies with different building layouts, Journal of the Air & Waste Management Association, 2009, 59(2): 196-206.

[3] Hua, Y., Wang, S., Wang, J., Jiang, J., Zhang, T., Song, Y., Kang, L., Zhou, W., Cai, R., Wu, D., Fan, S. Investigating the impact of regional transport on $PM_{2.5}$ formation using vertical observation during APEC 2014 Summit in Beijing. Atmospheric Chemistry & Physics, 2016, 16(24).

[4] Huang, R.J., Zhang, Y., Bozzetti, C., Ho, K.F., Cao, J.J., Han, Y., Daellenbach, K.R., Slowik, J.G., Platt, S.M., Canonaco, F., Zotter, P. High secondary aerosol contribution to particulate pollution during haze events in China, Nature, 2014, 514(7521): 218.

[5] Li, C., Fu, J., Sheng, G., Bi, X., Hao, Y., Wang, X., Mai, B. Vertical distribution of PAHs in the indoor and outdoor $PM_{2.5}$ in Guangzhou, China, Building and Environment, 2005, 40(3): 329-341.

[6] Qin, X., Yan, H., Zhan, Z., Li, Z. Characterizing vegetative biomass burning in China using MODIS data, International journal of wildland fire, 2014, 23(1): 69-77.

[7] Reddy, M.S., Venkataraman, C. Inventory of aerosol and sulphur dioxide emissions from India. Part II—biomass combustion, Atmospheric Environment, 2002, 36(4): 699-712.

[8] Shen, Z., Cao, J., Zhang, L., Zhang, Q., Huang, R.J., Liu, S., Zhao, Z., Zhu, C., Lei, Y., Xu, H., Zheng, C. Retrieving historical ambient $PM_{2.5}$ concentrations using existing visibility measurements in Xi'an, Northwest China, Atmospheric Environment, 2016, 126: 15-20.

[9] Sun, Y., Song, T., Tang, G, Wang, Y. The vertical distribution of $PM_{2.5}$ and boundary-layer structure during summer haze in Beijing, Atmospheric Environment, 2013, 74: 413-421.

[10] Tian, Y.Z., Wang, J., Peng, X., Shi, G.L., Feng, Y.C. Estimation of the direct and indirect impacts of fireworks on the physicochemical characteristics of atmospheric PM_{10} and $PM_{2.5}$, Atmospheric Chemistry and Physics, 2014, 14(18): 9469-9479.

 DOI: https://doi.org/10.30564/jasr.v3i2.2134

[11] Wang, J., Ho, S.S.H., Cao, J., Huang, R., Zhou, J., Zhao, Y., Xu, H., Liu, S., Wang, G., Shen, Z., Han, Y. Characteristics and major sources of carbonaceous aerosols in $PM_{2.5}$ from Sanya, China, Science of the Total Environment, 2015, 530: 110-119.

[12] World Health Organization. WHO Air quality guidelines for particulate matter, ozone, nitrogen dioxide and sulfur dioxide-Global update 2005-Summary of risk assessment. Geneva: WHO, 2006

[13] Wu, Y., Liu, J., Zhai, J., Cong, L., Wang, Y., Ma, W., Zhang, Z., Li, C. Comparison of dry and wet deposition of particulate matter in near-surface waters during summer, PloS one, 2018, 13(6): e0199241.

[14] Yang, Y., Liu, X., Qu, Y., An, J., Jiang, R., Zhang, Y., Sun, Y., Wu, Z., Zhang, F., Xu, W., Ma, Q. Characteristics and Formation Mechanism of Continuous Hazes in China: A Case Study in Autumn of 2014 in the North China Plain, Atmospheric Chemistry & Physics, 2015, 15: 8165-8178.

[15] Zhang, G., Li, J., Li, X.D., Xu, Y., Guo, L.L., Tang, J.H., Lee, C.S., Liu, X., Chen, Y.J. Impact of anthropogenic emissions and open biomass burning on regional carbonaceous aerosols in South China, Environmental pollution, 2010, 158(11): 3392-3400.

DOI: https://doi.org/10.30564/jasr.v3i2.2134

Author Guidelines

This document provides some guidelines to authors for submission in order to work towards a seamless submission process. While complete adherence to the following guidelines is not enforced, authors should note that following through with the guidelines will be helpful in expediting the copyediting and proofreading processes, and allow for improved readability during the review process.

Ⅰ. Format

- Program: Microsoft Word (preferred)
- Font: Times New Roman
- Size: 12
- Style: Normal
- Paragraph: Justified
- Required Documents

Ⅱ. Cover Letter

All articles should include a cover letter as a separate document.

The cover letter should include:

- Names and affiliation of author(s)

The corresponding author should be identified.

Eg. Department, University, Province/City/State, Postal Code, Country

- A brief description of the novelty and importance of the findings detailed in the paper

Declaration

v Conflict of Interest

Examples of conflicts of interest include (but are not limited to):

- Research grants
- Honoria
- Employment or consultation
- Project sponsors
- Author’s position on advisory boards or board of directors/management relationships
- Multiple affiliation
- Other financial relationships/support
- Informed Consent

This section confirms that written consent was obtained from all participants prior to the study.

- Ethical Approval

Eg. The paper received the ethical approval of XXX Ethics Committee.

- Trial Registration

Eg. Name of Trial Registry: Trial Registration Number

- Contributorship

The role(s) that each author undertook should be reflected in this section. This section affirms that each credited author has had a significant contribution to the article.

1. Main Manuscript
2. Reference List
3. Supplementary Data/Information

Supplementary figures, small tables, text etc.

As supplementary data/information is not copyedited/proofread, kindly ensure that the section is free from errors, and is presented clearly.

Ⅲ. Abstract

A general introduction to the research topic of the paper should be provided, along with a brief summary of its main results and implications. Kindly ensure the abstract is self-contained and remains readable to a wider audience. The abstract should also be kept to a maximum of 200 words.

Authors should also include 5-8 keywords after the abstract, separated by a semi-colon, avoiding the words already used in the title of the article.

Abstract and keywords should be reflected as font size 14.

Ⅳ. Title

The title should not exceed 50 words. Authors are encouraged to keep their titles succinct and relevant.

Titles should be reflected as font size 26, and in bold type.

Ⅳ. Section Headings

Section headings, sub-headings, and sub-subheadings should be differentiated by font size.

Section Headings: Font size 22, bold type

Sub-Headings: Font size 16, bold type

Sub-Subheadings: Font size 14, bold type

Main Manuscript Outline

Ⅴ. Introduction

The introduction should highlight the significance of the research conducted, in particular, in relation to current state of research in the field. A clear research objective should be conveyed within a single sentence.

Ⅵ. Methodology/Methods

In this section, the methods used to obtain the results in the paper should be clearly elucidated. This allows readers to be able to replicate the study in the future. Authors should ensure that any references made to other research or experiments should be clearly cited.

Ⅶ. Results

In this section, the results of experiments conducted should be detailed. The results should not be discussed at length in

this section. Alternatively, Results and Discussion can also be combined to a single section.

Ⅷ. Discussion

In this section, the results of the experiments conducted can be discussed in detail. Authors should discuss the direct and indirect implications of their findings, and also discuss if the results obtain reflect the current state of research in the field. Applications for the research should be discussed in this section. Suggestions for future research can also be discussed in this section.

Ⅸ. Conclusion

This section offers closure for the paper. An effective conclusion will need to sum up the principal findings of the papers, and its implications for further research.

Ⅹ. References

References should be included as a separate page from the main manuscript. For parts of the manuscript that have referenced a particular source, a superscript (ie. [x]) should be included next to the referenced text.

[x] refers to the allocated number of the source under the Reference List (eg. [1], [2], [3])

In the References section, the corresponding source should be referenced as:

[x] Author(s). Article Title [Publication Type]. Journal Name, Vol. No., Issue No.: Page numbers. (DOI number)

Ⅺ. Glossary of Publication Type

J = Journal/Magazine

M = Monograph/Book

C = (Article) Collection

D = Dissertation/Thesis

P = Patent

S = Standards

N = Newspapers

R = Reports

Kindly note that the order of appearance of the referenced source should follow its order of appearance in the main manuscript.

Graphs, Figures, Tables, and Equations

Graphs, figures and tables should be labelled closely below it and aligned to the center. Each data presentation type should be labelled as Graph, Figure, or Table, and its sequence should be in running order, separate from each other.

Equations should be aligned to the left, and numbered with in running order with its number in parenthesis (aligned right).

Ⅻ. Others

Conflicts of interest, acknowledgements, and publication ethics should also be declared in the final version of the manuscript. Instructions have been provided as its counterpart under Cover Letter.

BILINGUAL PUBLISHING CO.
Pioneer of Global Academics Since 1984

Journal of Atmospheric Science Research

Aims and Scope

Journal of Atmospheric Science Research publishes original research papers that offers a rapid review and publication that freely disseminates research findings in areas of Remote Sensing, Weather Extremes, Air Pollution, Satellite Meteorology and more. The Journal focuses on innovations of research methods at all stages and is committed to providing theoretical and practical experience for all those who are involved in these fields.

Journal of Atmospheric Science Research aims to discover innovative methods, theories and studies in all aspects of Atmospheric Science by publishing original articles, case studies and comprehensive reviews.

The scope of the papers in this journal includes, but is not limited to:

- Remote Sensing
- Climate Dynamics
- Air Chemistry
- Hydrological Cycle
- Satellite Meteorology
- Ocean Dynamics
- Climate Change
- Weather Extremes
- Air Pollution
- Weather and Climate Prediction
- Climate Variability

Bilingual Publishing Co. (BPC)

Tel:+65 65881289

E-mail:contact@bilpublishing.com

Website:www.bilpublishing.com

About the Publisher

Bilingual Publishing Co. (BPC) is an international publisher of online, open access and scholarly peer-reviewed journals covering a wide range of academic disciplines including science, technology, medicine, engineering, education and social science. Reflecting the latest research from a broad sweep of subjects, our content is accessible world-wide——both in print and online.

BPC aims to provide an analytics as well as platform for information exchange and discussion that help organizations and professionals in advancing society for the betterment of mankind. BPC hopes to be indexed by well-known databases in order to expand its reach to the science community, and eventually grow to be a reputable publisher recognized by scholars and researchers around the world.

BPC adopts the Open Journal Systems, see on ojs.bilpublishing.com

Database Inclusion

Asia & Pacific Science Citation Index

Creative Commons

China National Knowledge Infrastructure

Google Scholar

Crossref

MyScienceWork

BILINGUAL
PUBLISHING CO.
Pioneer of Global Academics Since 1984

Tel:+65 65881289
E-mail:contact@bilpublishing.com
Website:www.bilpublishing.com